AN ABSTRACT OF THE THESIS OF

Brian Koch for the degree of Master of Science in Electrical and Computer Engineering

presented on August 25, 1997. Title: **Characterization Studies and Industrial**

Control Development for the Brushless Doubly Fed Machine.

Redacted for Privacy

Abstract approved : _____

René Spée

This thesis presents the development of a supervisory controller for a pre-commercial Brushless Doubly-Fed Machine (BDFM) drive system. In addition, characterizations of new diecast rotors for the BDFM are presented. Using the characterization results from the new rotors, a control scheme was developed to allow a BDFM to be packaged into an integrated drive system, which is specific to the doubly-fed nature of this machine. Experimental evaluation of the diecast rotors indicates that this form of rotor production can be applied to BDFMs and allows for mass production at reasonable cost.

The control system was integrated within the BDFM drive system, making the first self-contained BDFM drive a reality. Since this drive is intended to be a prototype for commercial development, this thesis contains a detailed account of the supervisory control, how it was implemented, and how it can be operated or reconfigured. This controller has a number of functions, including: host for the user interface, synchronization control, speed control, ensuring optimum performance, and establishing active power factor correction.

Characterization Studies and Industrial Control Development
For the Brushless Doubly-Fed Machine

by

Brian Koch

A THESIS

submitted to

Oregon State University

in partial fulfillment of
the requirements for the
degree of

Master of Science

Presented August 25, 1997
Commencement June 1998

Master of Science thesis of <u>Brian Koch</u> presented on <u>August 25, 1997</u>

APPROVED:

Redacted for Privacy

Major Professor, representing Electrical and Computer Engineering

Redacted for Privacy

Chair of Department of Electrical and Computer Engineering

Redacted for Privacy

Dean of Graduate School

I understand that my thesis will become part of the permanent collection of Oregon State University libraries. My signature below authorizes release of my thesis to any reader upon request.

Redacted for Privacy   11/20/97

Brian Koch, Author

Characterization Studies and Industrial Control Development for the Brushless Doubly Fed Machine

TABLE OF CONTENTS

TABLE OF CONTENTS (continued)

LIST OF FIGURES

LIST OF TABLES

LIST OF APPENDICES

page

LIST OF APPENDIX FIGURES

Characterization Studies and Industrial Control Development for the Brushless Doubly Fed Machine

1. Introduction

This thesis presents the characterization of a pre-commercial Brushless Doubly-Fed Machine (BDFM) prototype, as well as the development of an outer loop, industrial controller for this machine. This chapter will include an explanation of the concept of the BDFM (sec. 1.1), as well as a historic overview (sec. 1.2) of the BDFM project, as it comes to a close at Oregon State University.

1.1 BDFM Concepts

With the growing popularity of variable speed drives in industrial applications which once relied on constant speed machines, there has been an increased desire to make the installation and operation of these drives more cost effective. This trend, combined with recent advances in power electronics, has led to the gradual replacement of the historically dominant DC drives with AC induction motor (IM) drives. IM drives have three significant advantages over DC machines in that they are less expensive, more robust as a result of the absence of a commutator, and require less maintenance. The major disadvantage of induction machine drives, compared to direct line connected IMs, is their high cost due to the power electronic converters required for variable speed operation. A number of techniques have been investigated to reduce the rating and cost

of the converters used in drives; some of these will be discussed in the literature survey in section 1.2.

The BDFM concept has reemerged to meet the demand for an ASD system with a converter rating that is significantly smaller than that of a comparable induction machine drive. The BDFM was derived from a system of two induction machines on the same shaft with a rotor that links the two stators. This self cascaded induction machine system can operate as an adjustable speed drive by varying one machine stator winding frequency [1]. Such a system requires a specialized and complex wound rotor to cascade the system. This makes the system much more complex and costly than an induction machine; moreover, this system will generally be much larger than a comparable induction machine.

The single frame BDFM was adapted at Oregon State University for use as an ASD in the late 1980's, to show that a variable speed drive could be manufactured with a significantly smaller converter rating. Figure 1.1 shows a converter connected to one set of the three phase winding. This winding set will be referred to as the "control winding" for the remainder of this thesis, since only a small portion of the power is passed though this set of windings, and the speed control of the machine is accomplished using this converter. Since the converter processes only a portion of total machine power, the converter has a lower rating and is significantly less costly. The other set of windings is connected directly to the utility service and is therefore operated at 60 Hz. This winding is referred to as the "power winding" since the majority of the power is passed through this winding.
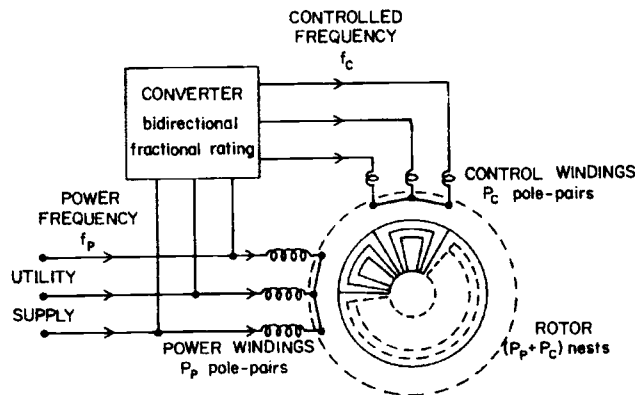
Figure 1. 1 BDFM drive system

Equal pole pair numbers for these windings are not used, in order to prevent transformer coupling between the windings and to ensure that all coupling flux will pass through the rotor. There are specific pole pair combinations that can be selected to assure balanced power transfer between the stator and the rotor. The laboratory prototype used in the ASD being developed was implemented with a 3/1 pole pair combination. The control winding is the 2 pole winding, while the power winding is the 6-pole.

The specialized cage rotor structure of the BDFM consists of a number of identical sections, or nests, equal to the sum of the pole pairs of the two stator windings [2]. Unlike in a conventional IM, the rotor bars are only shorted at one end of the stack. The other "endring" requires a selective connection of rotor bars. The bars are connected such that any given loop will connect two slots that have equal but opposite currents [3,4]. It has been shown in [3] that some slots in each nest do not contribute significantly

to the linkage between the stator and the rotor, which has led to their removal in the more recent machines produced at OSU in order to allow for a simple caged rotor. The specialized structure of the rotor enables the BDFM to operate in a synchronous mode, with both stator fields linked by the rotor. Recently, it has been demonstrated that the specialized cage rotor can be diecast with techniques common to induction machine rotor casting [5].

Generally, the two stator windings are excited with different frequencies and possibly different phase sequences. These two different excitations generate two air gap electromagnetic flux frequencies which lead to rotor currents of two frequencies when the machine is not operating in the synchronous mode. When the rotor speed is such that the flux frequency seen by the rotor from both stator windings is equal, the machine is locked in the synchronous condition, which allows for full power transfer from the stator to the rotor. The rotor mechanical frequency is related to the stator frequencies and pole-pair numbers by the following equation.

$$f_{mech} = \frac{f_p \pm f_c}{P_c + P_p} \qquad (1.1)$$

The subscripts $_p$ and $_c$ refer to power and control windings, respectively.

Comparisons between the BDFM and other machines for ASD applications show that the BDFM has a number of advantages. Because of the cage rotor structure and the lack of slip rings the BDFM is more robust, requires less maintenance and is less costly than a wound rotor induction machine. The power converter needed for a BDFM is smaller that the converter required for induction or synchronous machines and will be

cheaper than a converter for these machines. However, it requires an active rectifier stage, which is also useful to eliminate harmonic pollution on the utility grid. The smaller converter, coupled with the newly proven cast rotor technology, makes the cost of a BDFM system competitive with induction machine ASDs. The synchronous operation of the BDFM, along with the ability to control power factor and efficiency, makes it more versatile and very simple to control for relatively low performance systems. A BDFM is also more tolerant to converter tripping, since the loss of the converter will only affect the control winding and power may still be processed through the power winding for singly-fed, induction mode operation at a reduced power level.

1.2 Literature Survey

It was shown in 1907 by Hunt [1] that two independent stators could be combined into one frame to produce a doubly fed machine with no slip rings. A more effective stator and rotor design was then developed by Creedy [6] for this system. The idea of using a caged rotor structure to further simplify the machine was presented by Broadway [7] in the 1970's.

A number of researchers have investigated dynamic speed control of the BDFM, leading to the development of both scalar and field oriented control methods. Scalar control of the BDFM has taken a number of forms, beginning with open loop volts/Hz control [8,9], since the control winding frequency is directly related to the shaft speed in synchronous operation. Constant current control [10] has also been investigated and has the benefit of simplifying the control of 6-pole power factor. Closed loop scalar control

has also been investigated [11], but this has the disadvantage of requiring a costly speed transducer and does not improve the speed performance significantly over an open loop system. All scalar control approaches to speed control of the BDFM are applicable to slow speed response applications, such as pumps or fans [12, 13].

W.R. Brassfield [14, 15] developed a direct torque control algorithm but due to the complexity of the calculations involved, this algorithm was shown to be very limited in its practical usefulness [11]. D. Zhou developed a simplified torque controller based on the synchronous reference frame and field oriented control, which achieves a speed response in the order of 200 r/min per second but requires a costly position sensor [11].

Work on doubly-fed concepts has also been applied to other machine platforms. Industrial implementation of slip power recovery ASDs or variable speed generation using wound rotor induction machines has occurred [16]. These systems have the problem of an expensive rotor as well as requiring regular maintenance. The doubly-fed reluctance machine is also being researched, but its specialized rotor is very complex in comparison to the BDFM [17].

1.3 Thesis Outline

This thesis consists primarily of two main parts: the characterization of the machine with the new diecast rotors and the control development for use with a converter designed at OSU for the BDFM [18]. The BDFM project has been carried through to the point where manufacturing of a cost effective ASD is the major focus of the current work. Successful diecasting of BDFM rotors has been demonstrated and is reported in

[5]. Characterization of the rotor/stator combination was carried out to evaluate the casting process and to obtain detailed information on machine performance to be used in the control development. The characterization of the machine is described in Chapter 2.

In parallel with the work reported here, a bi-directional converter was developed for use with the BDFM. This converter has a number of special features that allow a BDFM to be operated from a single self-enclosed device. Using the knowledge gained from characterization, a controller was developed as an integral part of the drive, to be enclosed with the converter. Because of the BDFM's synchronous nature and cost considerations, the speed control loop is scalar and open loop. A power winding current feedback loop is incorporated into the control to allow for the tuning of a performance parameter at different speeds and loads. The development, implementation, and performance of the controller are described in chapters 3 and 4, while results are given in chapter 5 and chapter 6 lists conclusions and recommendations.

2. Characterization of the 5hp Cast Rotor BDFM

To characterize the BDFM with new diecast rotors, each rotor was tested extensively in the same stator, and compared with a benchmark rotor that was manufactured using copper bars instead of diecast aluminum [19]. The following tests were performed for each rotor:

- Open-circuit test to determine the saturation characteristics of the machine;

- Run-up test, with the control windings both open and short circuited, to investigate the dynamic induction mode characteristics of the rotors;

- Steady-state induction mode tests with the control windings either open or short circuited, to investigate parasitic currents in the rotor;

- Open circuit variable speed tests to evaluate the magnetic linkage between the two stator windings, and to evaluate non-desirable harmonics;

- Synchronous-mode tests, with a number of different loads to look at performance.

2.1 Considerations and Methods for Diecasting BDFM Rotors

In order to avoid inter-bar current leakage and the associated undesired induction torque components, good insulation between rotor stack and bars is required. If currents are allowed to flow across the stack from bar to bar, a single rotor frequency will not be ensured and induction torque will develop. Inter-bar, laminar rotor currents result in a parasitic rotor cage effect which in turn causes destabilizing torque components.

In addition to undesirable IM torque, the inter-bar currents also lead to additional I^2R loss. As the stator to rotor slip frequency increases, the inter-bar voltage will increase. This in turn increases parasitic currents passing through the rotor laminations, causing localized rotor heating. This has been seen as localized heat discoloration of the rotor stack on the less successful rotors. It also leads to induction torque which the synchronous BDFM must compensate for, effectively changing the mechanical load. The 6-pole slip will produce an accelerating torque in an attempt to increase the speed of the rotor to 1200 r/min (synchronous speed for a 6-pole machine excited with a 60 Hz supply). Under high load operation, the parasitic 6-pole induction torque adds to the BDFM torque and allows it to support higher loads for short periods of time, but under low torque loads the parasitic IM may cause loss of synchronism if the BDFM cannot retard the accelerating effects.

Previous research has produced working BDFMs based on a manufactured rotor [19]. The rotor of this machine was custom manufactured using laser cut laminations and insulated copper bars. This machine compared favorably to an 8-pole induction machine with regards to efficiency for pump and fan applications[19]. Since the characteristics of this BDFM are known and compare well with IMs, its rotor was used as a benchmark for comparison to the diecast rotors considered in this study.

In order to investigate diecasting feasibility, laminations for ten new rotor stacks were custom manufactured from insulated silicon steel by laser cutting. These rotor stacks are designed to have the same outside diameter and stack length as the benchmark rotor in order to be used in the same stator. The rotor slots are closed to allow for

diecasting without a retaining sleeve. The rotor slot area is increased such that the aluminum rotor bars have the same effective resistance as the copper bars of the baseline rotor. In an attempt to accommodate the larger bars without drastically changing the magnetic circuit, the bar shape was changed from round to trapezoidal, leaving the distance between rotor bars unchanged from the benchmark rotor. A drawback of the trapezoidal shape is the possibility of saturation, which was indeed observed in testing. The number of slots and the slot pitch were left unchanged (40 and 9^0, respectively). Unlike the manufactured rotor, which has straight bars, the cast rotor bars are skewed by one stator slot to reduce slot harmonics and cogging torque caused by straight bars.

Four different precasting stack preparation methods were investigated in this study:

A) The first preparation was no treatment other than exposure to handling and the environment during shipping. This provides a second baseline for comparison with the other preparations. At best, these rotors have a thin layer of iron oxide in the slots to provide insulation between the bars and the stack.

B) The second preparation method was to heat the uncast stack in an atmosphere containing Sulfur Hexafluoride to produce an insulation layer of Iron Fluoride on all exposed metal surfaces. This treatment can be combined with the preheating of rotor stacks prior to diecasting. This coating has a high contact resistance (in the order of $M\Omega$), but does not hold up well to the rigors of casting at high pressure, as some flaking during casting may occur. This plating process may also be eroded chemically by the molten Aluminum if the Fluorine is attracted to the Aluminum.

C) The third preparation was to dip the rotors in an Iron Oxide slurry coreplate used in the production of some IM rotors. This yields a coating of the entire rotor stack, including the insides of the rotor slots and the ends of the stack. However, because of curing or dilution deficiencies this treatment may cause gas bubbles to form in the aluminum bars during casting. Several attempts at coreplating were made using a variation of dilution, curing temperature, and curing duration, thus attempting to strike an acceptable compromise for a sufficient coating while minimizing out-gassing.

D) The fourth treatment was to heat the rotors in a moist environment to induce rusting on the exposed metal surfaces. This is the simplest of the treatments and can be combined with necessary preheating of the rotors before casting.

The rotors were diecast in a vertical diecasting machine. The molds for the process were machined from 4140 carbon steel, instead of a harder die material, due to the short production run of 10 rotors. 99.7% pure Aluminum heated to $1250°$ F was the agent being cast. The cavity inlets to the mold are designed using basic fluid equations to achieve a good fill factor. The casting was done at relatively high pressure (4000 psi, causing velocities of 31 in/sec on the aluminum) to ensure adequate bar fill, since the small sample size allows for almost no experimentation with combinations of pressure and temperature. The high casting pressure may have caused more erosion of all core treatments than casting at normal industrial pressure would.

As with conventional IMs, the rotor's outside diameter is turned down to size on a lathe after casting and mounting. Machining was done in two passes, one from each end of the rotor, in order to minimize shorting of the laminations at the surface of the rotor.

After the rotors were machined to size and tested, one sample of each stack preparation was quenched in order to investigate the effects on stack to bar insulation. The rotors were quenched after testing to establish pre and post-quenching performance. Quenching was performed by heating the rotors to 900° F , below the annealing point of the stack laminations, and then cooling. Due to the different coefficients of expansion of the steel laminations and aluminum bars, this process separates the bars from the stack. Quenching techniques are also commonly applied in IM manufacturing.

2.2 Experimental Facility

The testing system for the BDFM has been used extensively in the past [11, 19]. The test load is a DC machine drive that can either be controlled manually or via computer to emulate different torque speed characteristics, and thus different loads. The BDFM and the load are mounted on a steel frame with all the necessary attachments for alignment. Shaft torque and speed are measured with a shaft-mounted Himmelstein transducer. The electrical measurements were conducted using a bank of power, RMS current and RMS voltage traducers. The test data was gathered from the torque and RMS transducers using computerized instrumentation, as well as a BMI power analyzer and a 400 MHz Tektronix oscilloscope. Power was supplied to the 6-pole power winding of the machine either from the Dearborn Hall 230/115 volt 60 Hz grid, or through a 3-phase variac if the test required a variable voltage. The 2-pole control winding received power from an EPC current regulator.

2.3 Open-Circuit Tests

2.3.1 Benchmark power winding saturation test

In order to observe saturation in the power winding's magnetic circuit, the benchmark manufactured rotor was driven at 1200 r/min by the DC drive used in an open loop configuration. The 6-pole power winding voltage was varied between 0 V and its rated voltage via the variac from the 60 Hz building supply while the current was observed. As can be seen from Figure 2.1, the 6-pole power winding magnetic circuit does not appear to saturate with a 60 Hz supply.
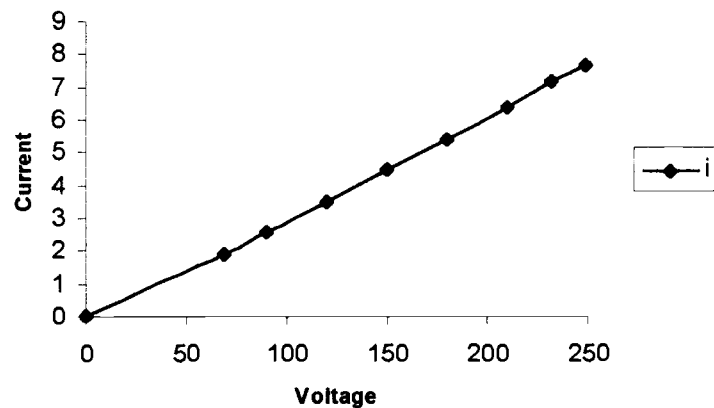
Figure 2. 1 Power winding saturation with benchmark rotor (Current in A, Voltage in V)

2.3.2 Cast rotor saturation

The cast rotors exhibited a different saturation curve than the benchmark rotor even though the air-gap was essentially the same. This can possibly be attributed to the slot shape and skewing of the rotor bars. Comparison between all the cast rotors showed they all had approximately the same saturation curves, since at synchronism, the rotor circuits are electrically removed from the circuit. As shown in Figure 2.2, the 6-pole power winding curve showed some saturation at approximately 100 volts but the saturation is not steep. Instead of the 8 A of magnetizing current seen with the benchmark rotor at 250 V, over

9 A is seen with the cast rotors. This was a 13% increase in the magnetizing current caused by the saturation of the cast rotors. As a result of the trapezoidal bar shape and localized tooth saturation.
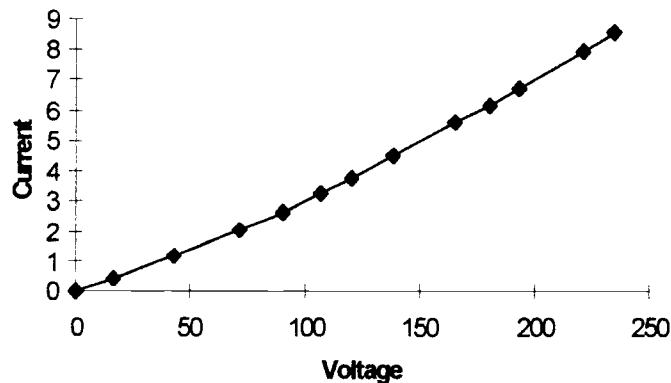
Figure 2. 2 Power winding saturation with cast rotors (Current in A, Voltage in V)

2.3.3 Benchmark rotor control winding saturation test

Saturation of the 2-pole control winding magnetic circuit was observed in a similar manner. The rotor was driven at 1200 r/min by the DC drive. With the EPC converter set at 20 Hz, the 2-pole control winding voltage was varied between 0 volts and a voltage that produced rated current. It can be seen from the graph shown in Figure 2.3 that the 2-pole control winding saturates at approximately 2 A, 125 V.
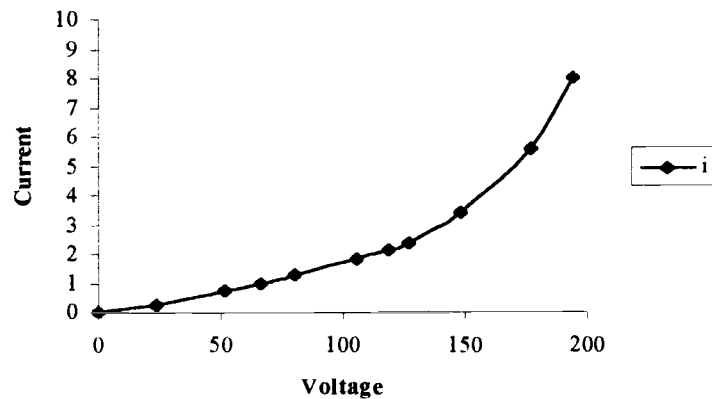
Figure 2. 3 Control winding saturation with benchmark rotors
(Current in A, Voltage in V)

2.3.4 Cast rotor control winding saturation tests

The control winding saturation did not change significantly for the cast rotors. The pole span of the control winding is three times larger than that of the power winding, so the skewed bars have little effect on the control saturation. The back iron saturation is still the

dominant effect of the control winding saturation at 20 Hz. Again, all of the cast rotors

showed the same saturation.
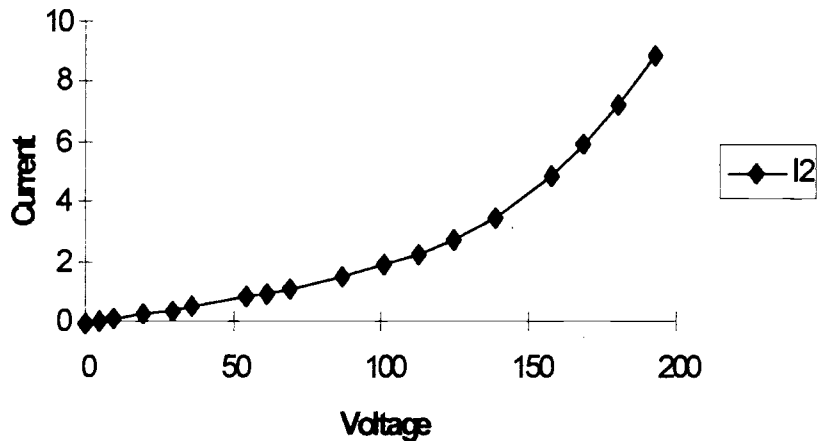
Figure 2. 4 Control winding saturation with cast rotors (Current in A, Voltage in V)

2.4 Run-up Curves

2.4.1 Open control winding

This test was conducted in order to observe the run-up characteristics of the lab

BDFM. The machine was started from standstill by simply closing the 230 V contactor to

the power winding, while the control winding was open circuited. The Tek 400 MHz scope

was used to observe speed, torque, and current wave forms during run-up of the machine.

2.4.1.1 Benchmark rotor:

The peak startup current for the benchmark rotor in the open circuit induction mode was at approximately 14A. The torque peaked a 113 LB-in (12.83 Nm) immediately following energization. There was a small torque cusp at speeds above 900 r/min, followed by a torque peak as the speed approached 1200 r/min. At a speed just below 1200 r/min, the average torque level dropped to the point where the machine would no longer accelerate. Once the machine reached steady state, the torque signal oscillated at 20 Hz. The same test was then repeated, except that the 2-pole control winding induced voltage was monitored instead of the 6-pole power winding current. At stand still, the induced voltage was near 245 V peak line to line and decreased steadily as the speed increased.

2.4.1.2 Cast rotors:

All the cast rotors had significantly higher startup torque in the open control winding induction mode than the benchmark rotor. The leakage between the nested bars allowed the rotor to have an induction machine like start up characteristic. The rotors with better insulation started with less torque but all accelerated much faster than the benchmark rotor's startup time of 14 seconds. Table 2.1 details the open control winding startup characteristics for the different cast rotors. The data shown may be affected by under-sampling with the digital oscilloscope caused by the long sampling time. Appendix 1 shows examples of the run-up curves.

Table 2. 1 Open control winding run-up characteristics

Rotor	Time to 1200 r/min (sec)	Peak 6P current (A RMS)	Peak 2P Voltage (V peak)	Steady State 6p Current (A RMS)	Max. Torque (LB-in)
Benchmark	14.0	14	245	6.5	113
Untreated	1.6	30	220	8.7	495
FeF2	1.0	28	180	8.7	575
Dipped	2.5	25	300	8.7	407
Rust	1.3	26	250	8.7	540
Untreated Quenched	2.0	28	250	8.8	480
FeF2 Quenched	3.0	20	250	8.6	426
Dipped Quenched	3.0	20	300	8.6	340
Rust Quenched	3.0	20	250	8.6	420

2.4.2 Short-circuited control winding

This test was similar to the previous test except the 2-pole control winding was short-circuited by a copper bar at the instrumentation rack. This test was done in two parts like the previous test; the first to read the 6-pole power winding current wave form along with the torque and speed signals, the second to view the 2-pole control winding current.

2.4.2.1 Benchmark rotor:

As expected, the start up torque was much higher (~47 Nm) than during the open control winding tests. Also, as expected, the torque was observed to drop to zero when the speed reached 900 r/min. The 6-pole power winding current reached ~28 A during start up and settled to ~12 A once the machine reached steady state at 900 r/min. The test was then

repeated in order to observe the 2-pole control winding current. The 2-pole control winding current was constant at 12 A during the majority of the run-up, with a decreasing frequency as the machine accelerated to 900 r/min. As the speed nears 900 r/min, the 2-pole control winding current frequency decreases sharply as the current becomes DC and goes to zero.

2.4.2.2 Cast rotors:

The short circuit run-up characteristics of the cast rotors more closely resembled the benchmark rotor than for the open circuit test. Some of the rotors showed some over shoot of the 900 r/min synchronous point. The following table lists the characteristics of the different cast rotor run-ups. The results are prone to measurement error since the digital oscilloscope was being under-sampled to get the electrically long run-ups; nonetheless, they show the basic trends. See Appendix 1 for examples of the run-up curves.

Table 2. 2 Open control winding run-up characteristics

Rotor	Time to Steady State	Final Speed (r/min)	Peak 6P Current (A RMS)	Peak 2P Current (A RMS)	Steady State 6P Current (A RMS)
Benchmark	.60	900	28	12	12
Untreated	0.48 sec	928	28	15	16
FeF2	0.44 sec	905	42	14	19
Dipped	0.58 sec	903	35	18	15
Rust	0.45 sec	904	40	15	19
Untreated Quenched	0.60 sec	904	35	19	15
FeF2 Quenched	0.60sec	902	31	17	14
Dipped Quenched	0.60 sec	902	35	20	14
Rust Quenched	0.60 sec	901	31	19	14

2.5 Steady State, Induction Mode Torque-Speed Test

For all of the steady state, induction mode torque-speed tests, the speed of the machine was controlled with the DC drive used in an open loop configuration. The torque-speed tests were only conducted over a range of speeds that keep the 6-pole power winding currents within rated limits at the various excitation levels. This was to prevent the machine from over heating at higher slips.

2.5.1 Benchmark rotor, shorted control winding torque/speed characterization

The torque-speed profile of the lab BDFM was taken using a 6-pole power winding excitation of 115 V, so a wider speed range could be observed. With the 2-pole control winding short-circuited, the major characteristic of the torque-speed curve was the negative torque seen between speeds of 900 r/min and ~1025 r/min. The torque-speed curve for the benchmark rotor along with the power current can be seen in Figure 2.5.
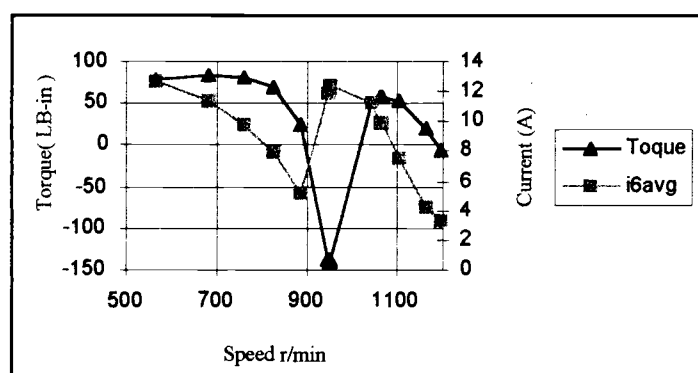
Figure 2.5 Shorted control winding induction characteristic for the manufactured rotor
(115 V 6-pole excitation)

2.5.2 Cast rotor, shorted control torque/speed characterization

The shorted control winding curves of the cast rotors are very similar to the 115V curves of the benchmark rotor. At the reduced excitation the saturation caused by the skewing and rectangular bars is not evident. The inter-bar current that would cause the rotors to appear as a caged rotor were only evident to a small extent in some of the worst performing rotors. This evidence indicates that all the cast rotors will act as BDFM rotors for a reduced excitation (also shown in the synchronous tests).

The untreated rotors had 45% less negative torque in the 900-1000 r/min range while their positive torque was higher in the 600-900 r/min range than the benchmark rotor as seen in Figure 2.6. Also, there is torque at 900 r/min where a true BDFM rotor would provide no torque in this configuration. The current of the 6-pole power winding was not significantly increased over this range but was higher by ~1 A at 900r/min. All these factors show that the untreated cast rotors have some interbar current that leads to an induction machine effect on the BDFM rotors. Minor heat markings on these rotors show some of the interbar bar current may have been flowing in localized areas of the rotor near the center nest of some of the endrings.
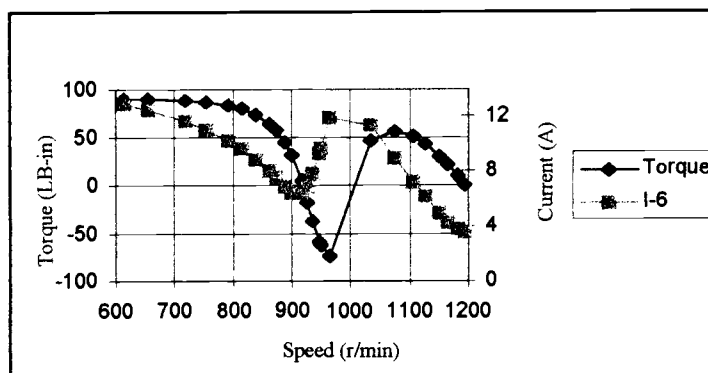
Figure 2.6 Shorted control winding induction characteristic for the untreated cast rotor
(115 V 6-pole excitation)

As shown in Figure 2.7, the iron-fluoride treated rotor fared no better than the

untreated rotors, and had similar torque and current curves, also due to interbar currents.

Heat marking on the fluoride rotors shows that the current flow through the rotor laminations

was distributed around the radius of the rotor in bands mostly close to the nested endrings but

in other locations as well.
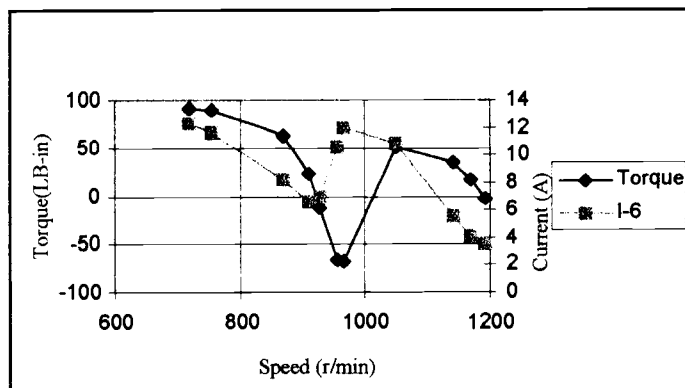
Figure 2.7 Shorted control winding induction characteristic for the fluoride treated rotor
(115 V 6-pole excitation)

The iron-oxide treated rotors were slightly better than the untreated rotors with

5 LB-in more negative torque and slightly lower peak torque in the sub 900 r/min speed

range. The torque at 900 r/min was also lower. There is still an indication of the induction

machine in these rotors but not as pronounced as in the untreated rotors. Results are shown

in Figure 2.8.
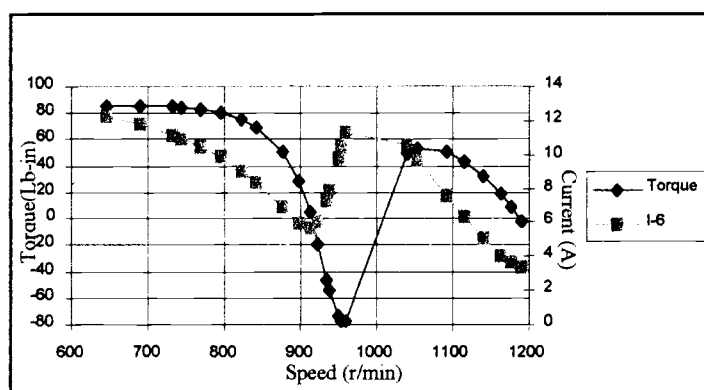
Figure 2. 8 Shorted control winding induction characteristic for the rusted rotors
(115 V 6-pole excitation)

As shown in Figure 2.9, the slurry dipped rotors had slightly better curves than the

rest of the unquenched rotors but still showed some induction machine characteristics.

Heating problems later degraded the rotor and highlighted the leakage current paths to be

into the center loop of the nested endrings.
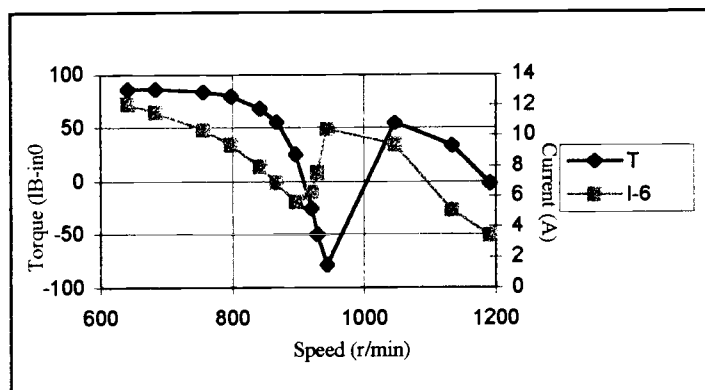
Figure 2. 9 Shorted control winding induction characteristic for the dipped rotors
(115 V 6-pole excitation)

The untreated and quenched rotor is a visible improvement over its unquenched twin.

The negative torque is larger, and the torque at 900 r/min is small but still present. The

quenching increased the insulation between the bars and the stack but did not make this rotor

a perfect BDFM. Results may be seen in Figure 2.10.
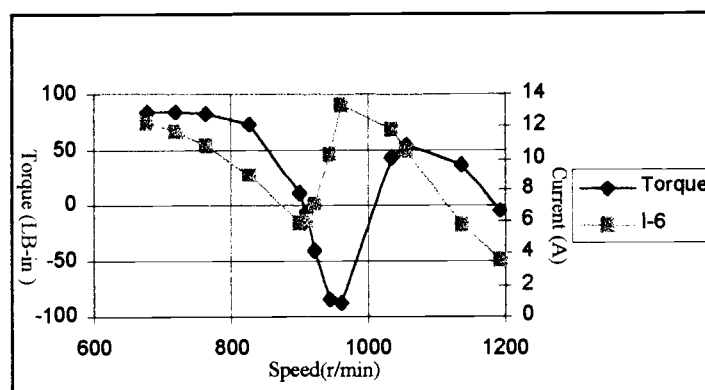
Figure 2. 10 Shorted control winding induction characteristic for untreated and quenched
rotor (115 V 6-pole excitation)

Figure 2.11 shows that the iron-fluoride and quenched rotor has characteristic curves that are very similar to the benchmark rotor. One exception is that higher currents are seen when the machine is producing its largest negative torque which is only 20 LB-in less than the benchmark rotor's peak negative torque.
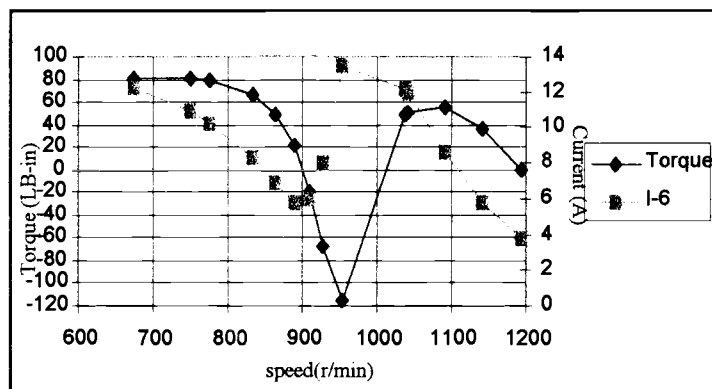
Figure 2. 11 Shorted control winding induction characteristic for the fluoride treated and quenched rotor (115 V 6-pole excitation)

The dipped rotor also improved dramatically after quenching, but did not demonstrate characteristics of the quality that the fluoride treated rotors had. As shown in Figure 2.12, the lowest recorded torque was only -101 LB-in compared to the -140 LB-in of the benchmark rotor.
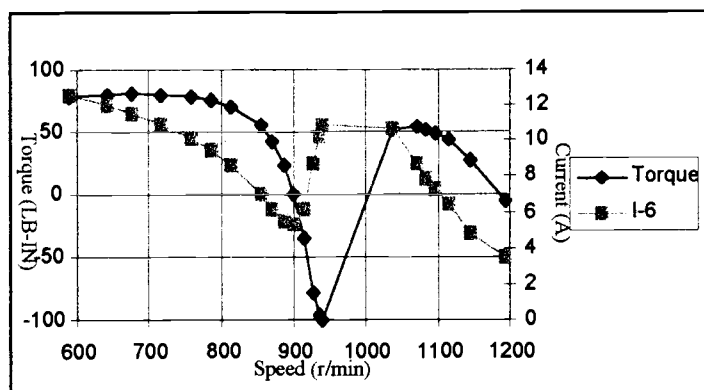
Figure 2. 12 Shorted control winding induction characteristic for the dipped and quenched rotor (115 V 6-pole excitation)

As seen in Figure 2.13, the rusted and quenched rotors perform very well, having a curve that matches the benchmark rotor more closely than any of the other rotors. While the critical most negative torque point is absent, the trend of the curve indicates that it has a negative torque characteristic slightly better than the quenched fluoride rotors.
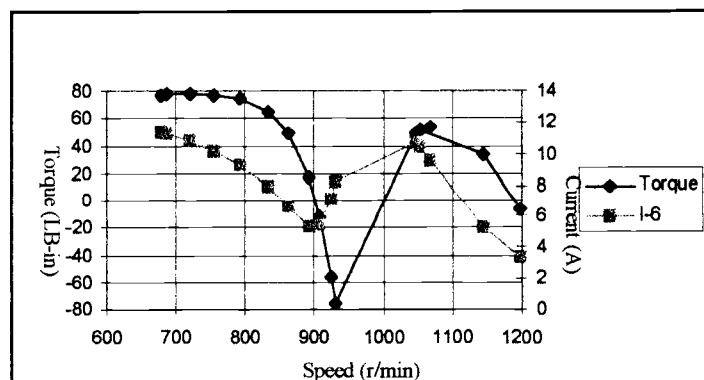
Figure 2. 13 Shorted control winding induction characteristic for the rusted and quenched rotor (115 V 6-pole excitation)

2.5.3 Open control winding characterization at reduced excitation

The torque-speed characterization was repeated with the control winding open circuited. With 115 V of excitation, the benchmark machine supported very little torque over a full range of slip. At these low levels of torque the transducer was affected by noise to some extent, but the torque trends are clearly visible in Figure 2.14. The benchmark rotor clearly has very little parasitic induction characteristic, an indication of good rotor bar insulation.

The untreated cast rotor had a significantly different induction mode characteristic than the benchmark rotor. Instead of the low levels of torque seen on the benchmark rotor through out the speed range, the torque increased to significantly higher levels at low speed as seen in Figure 2.14. The torque curve of this rotor is consistent with a high starting torque induction machine that would have similar rotor bar shapes to the BDFM rotor bars.

The iron-fluoride coated rotors had an even worse open control winding torque speed profile. The torque was higher over the speed range, indicating that the inter bar current in this rotor follow paths that allow for prevalent parasitic induction torque. Heat marking on this rotor indicated current flow around the rotor near the nested endrings. This may have been a possible result of the insulation on the rotors flaking off during casting.

The dipped rotors had a significantly better induction torque characteristic and could be operated near standstill without reaching excessive currents. This indicates that the insulation on the rotor bars of the dipped rotor is significantly better than the insulation of the

other cast rotors. This was proven by the fact that this was the only one of the cast rotors

that could be operated in the synchronous mode without quenching.

The rusted rotors have a very similar speed-torque profile to the fluoride coated

rotors but with slightly lower torque, indicating less parasitic induction effect.
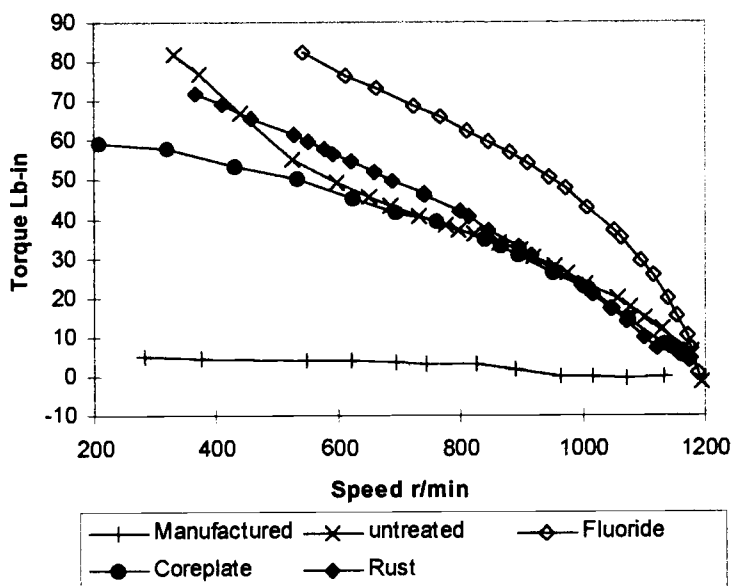
Figure 2.14 Open control winding induction torque-speed characteristic of the
unquenched cast rotors (115V 6-pole exitation)

Quenching significantly improved the characteristic of all the diecast BDFM rotors.

Figure 2.15 shows the torque-speed profiles of the quenched diecast rotors. The coreplated

rotor improved to the point of being nearly identical to the manufactured rotor,

supporting almost no torque throughout the speed range. Thus, quenching provides

enough insulation between the stack and bars and allows very little current to flow

between the nests of the coreplated and quenched rotors. The other rotors also benefited

significantly from quenching, allowing them all to be operated in the synchronous mode. As can be seen from Figure 2.15, the rusted and fluoride treated rotors have nearly identical characteristics and support little torque over the full speed range. The untreated rotor still supports significant induction torque and did not benefit as much from quenching since there was little insulation between the bars and the stack to begin with.
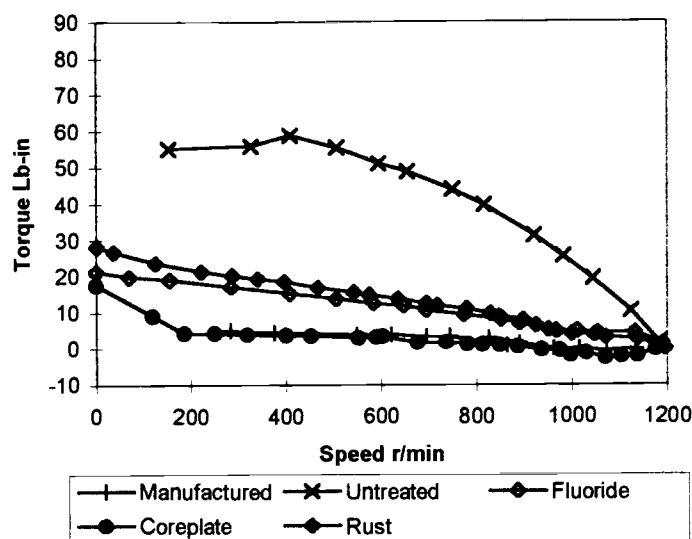
Figure 2.15 Open control winding induction torque-speed characteristic of the quenched cast rotors (115 V 6-pole excitation)

2.6 Open-Circuit 2-Pole Control Winding Voltage Waveforms

This test was conducted in order to observe the induced voltage on the control winding over the normal operating range of the machine. The BDFM was driven by the DC

drive while the power winding was excited though the variac at a reduced voltage. The control winding was left open-circuited and the voltage induced on it was monitored with a differential voltage probe attached to the Tek oscilloscope. Voltage and frequency spectrum wave forms were taken at 100 r/min increments between 500 and 1100 r/min.

For the benchmark rotor the major characteristic of the wave form was an AC induced voltage at the frequency required by a control current for synchronous operation at that speed. As was expected, the frequency of the induced voltage decreased to zero as the speed was increased to 900 r/min and then increased as the speed was changed from 900 to 1100 r/min. The second prominent feature of the waveform was a ripple on the induced voltage. As the speed of the machine increased the frequency of the ripple increased proportionately. This seems to indicate an effect caused by the straight rotor bars of the machine.

All the cast rotors had very similar included voltage characteristics because they all have the same bar shapes and skewing. The skewing of the rotor bars reduces the slot harmonic by 10 dB as compared to the benchmark rotors and effectively eliminates the second harmonic of the slot ripple. Examples of cast rotor wave forms can be seen in Appendix 2.

2.7 Synchronization Tests

This test was simply to observe if the BDFM would synchronize from stand still with no load for a limited speed range between 450 and 850 r/min. The test was conducted at

each speed by first putting a frequency on the 2-pole control winding that would cause the machine to run at the desired speed once it synchronized. If the 2-pole control winding current needed to synchronize the machine was high enough to rotate the BDFM, the 2-pole control winding current was used to brake the machine, after it was run-up with the 6-pole power winding, and the 6-pole power winding was connected when the rotor stopped turning. If the machine synchronized, the same procedure was conducted with a lower 2-pole control winding current at the same frequency in order to find the minimum control current for synchronization at each speed. Only some of the cast rotors were able to synchronize on the fly at 230 V and they are listed in Table 2.3. At higher speeds, the minimum control current for synchronization was found to be lower than the current required at lower speed.

Table 2. 3 Minimum synchronization current for cast rotors

	Benchmark	Dipped	Dipped Quenched	Rusted Quenched	Fluoride Quenched	Untreated Quenched
Speed (r/min)	min. current A	min. current A	min. current A	min. current A	min. current A	min. current A
850	1.3	5.1	2.1	4.8	3.0	3.3
800	3.7	5.0	3.7	7.6	6.1	6.6
700	6.5	7.7	4.4	7.8		
600	5.1	7.2	6.2			
550	6.8					
500	7.8					
450	7.2					

2.8 Synchronous Tests

For this test, computer control was used to command the DC drive to emulate various torque characteristics. Once the BDFM was synchronized, its performance was monitored at speeds between 600 and 900 r/min. At each speed, the control current was varied between its rated maximum and the minimum current required to keep synchronization. Data was collected using computerized data collection connected to the RMS instrumentation rack [19]. Two points of interest were focused on for each speed: the points of maximum efficiency and maximum power factor.

The various rotors were compared in the synchronous mode of BDFM operation. Performance, with both cubic and constant torque loads (emulated by the DC drive), was evaluated over the design speed range of 600-900 r/min. The following table shows some representative line-to-shaft efficiency results at the upper and lower speed and load points to illustrate the performance for the different stack preparation methods. The only unquenched rotors that were able to operate in the synchronous mode at full excitation were the slurry dipped rotors. All the rotors, including the untreated rotor, are able to operate in the 230 V synchronous mode after quenching. The dipped rotors have very promising efficiency at high speeds, but had higher rotor leakage currents at lower speeds. This in turn causes lower efficiency and excessive rotor heating at high torque levels. After quenching, the dipped rotors gained efficiency, with the difference being most noticeable at low speeds. The untreated and quenched rotor had the expected lower

efficiency at both low and high speeds. The rust and iron-fluoride treated rotors match almost identically with the edge going to the rusted rotor.

Table 2. 4 Synchronous parameters of the diecast rotors

	CUBIC TORQUE CHARACTERISTIC				
	speed (r/min)	2-pole current (A)	6-pole current (A)	Eff. %	PF %
Benchmark	850	8.0	10.0	71	88
	850	6.0	10.3	75	74
	800	7.5	8.0	67	80
	800	4.0	10.0	72	60
	600	8.3	6.6	34	52
	600	3.6	9.6	47	34
Dipped					
	850	8.0	9.9	64	85
	850	5.2	11.4	69	72
	600	7.2	9.2	25	52
	600	2.3	12.0	30	35
Dipped and Quenched					
	850	8.1	10.0	70	78
	850	5.7	11.7	74	65
	600	9.6	9.6	26	44
	600	2.7	11.7	41	32
Untreated and	850	7.8	10.7	68	77
Quenched	850	5.7	12.0	70	68
	600	7.3	10.6	20	52
	600	3.9	11.5	28	40
Quenched					
FeF_2	850	7.8	10.9	70	73
	850	6.4	11.7	72	66
	600	7.5	9.9	28	41
	600	3.6	11.7	38	31
Quenched	850	7.5	10.5	71	75
FeO_2	850	5.3	11.9	73	65
	600	7.5	8.7	28	44
	600	1.8	12.0	38	31

Table 2.4 continued

CONSTANT TORQUE CHARACTERISTIC 210 LB-in					
	speed (r/min)	2-pole current (A)	6-pole current (A)	Eff.	PF
Benchmark	550	8.0	9.0	57	77
	550	4.3	11.5	63	60
Dipped	Heating problems				
Dipped and Quenched	600	7.9	10.2	56	69
	600	5.4	11.7	60	60
Untreated and Quenched	600	7.8	10.6	52	70
	600	5.6	12.0	56	63
Quenched	600	8.0	10.6	49	70
FeF$_2$	600	6.0	11.9	56	62
Quenched	550	7.7	9.9	47	75
FeO$_2$	550	4.9	11.4	53	63
	600	7.7	10.0	51	75
	600	5.3	11.3	57	65

2.9 Characterization Conclusions

This chapter shows that a diecast BDFM can be produced that will work. The dipped rotors were shown to have efficiencies that were not far from the manufactured rotors. Due to the change in bar shape between the manufactured and diecast rotors, a direct comparison of efficiencies is not valid to indicate rotor losses. Skewing also reduces the effective magnetic coupling between stator and rotor fields, and the

trapezoidal bar shape leads to some localized saturation at the airgap. This saturation leads to higher magnetizing currents in the 6-pole winding for the diecast rotors. In order to establish a more meaningful basis of comparison, stator I^2R losses can separated from the total machine losses to produce an adjusted loss. The remaining power includes contributions due to iron losses of both the stator and the rotor, the I^2R losses of the rotor bars, bearing losses, windage, and the losses caused by inter-bar currents. At a given operating point, most loss components should be equal for manufactured and cast rotors, with the exception of inter-bar current losses, which are being investigated. Figures 2.16 and 2.17 show a comparison of the adjusted losses between the benchmark manufactured rotor and the dipped and quenched cast rotor for two different loads. As can been seen from these figures, the rotor losses for these two rotors are very similar at high speed.
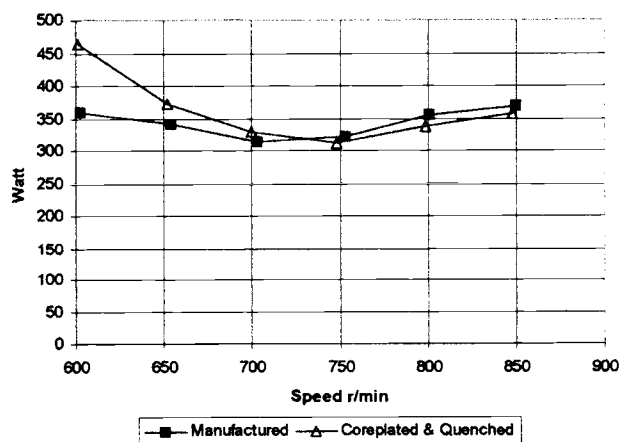
Figure 2.16 Comparison of rotor losses between the benchmark rotor and the dipped rotor for a cubic torque load
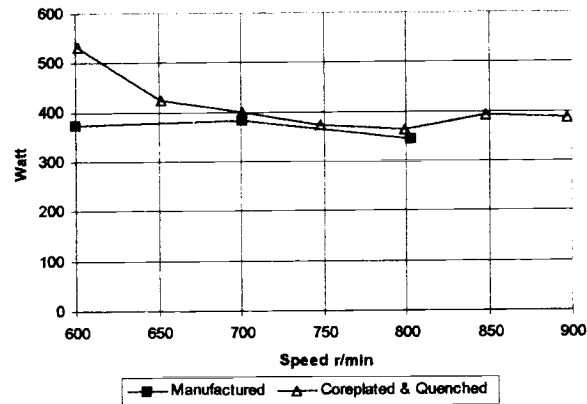
Figure 2.17 Comparison of rotor losses between the benchmark rotor and the dipped rotor for a constant torque load

This data proves that diecasting is feasible and will produce reasonable rotors if care is taken during design to allow for proper magnetic linkage between the rotor and the stator.

Not only does the data detailed in this chapter indicate the success and short comings of the diecast rotors, but it is also invaluable for development of a control system for the BDFM.

3. Control Development

The BDFM development program has focused on the possibility of using this machine in ASDs that are less costly than induction machine drives. With the requirement of a smaller power converter this seems practical, since the converter cost makes up over half of the cost of an induction drive system. A number of BDFM control techniques have been implemented, starting with scalar open-loop V/F and constant current control. These types of control are very useful for the BDFM because in synchronous operation the speed of the machine is directly related to the stator winding frequencies. Some work was done on closed-loop scalar control to remove the oscillatory response to a large step change in the control current frequency. This added a speed transducer to the system and was not as practical as simply slowing down the response of the control frequency to a change in speed command. More advanced forms of control for the BDFM have been implemented by Dongsheng Zhou [11], but most of these require extensive processing power and numerous transducers, including a costly position encoder.

For simplicity, the controller for the preproduction BDFM drive system is implemented with open loop scalar control using simple ramp changes in the control frequency. Along with speed control this controller has a primary function of controlling the contactors necessary for synchronization of the BDFM. Another function of the controller is to set the control current level to ensure synchronous operation as well as to provide for an efficient operating condition. The controller also operates as the host interface between the system and an industrial control terminal. The final task of the

controller is to command the rectifier to synthesize a leading current to partially make up for the lagging current of the power winding, thereby improving the power factor of the system. This chapter provides the theoretical and intuitive ground work for the control of the pre-production BDFM; the following chapter will outline the actual implementation and operation of the BDFM controller.

3.1 Control Applications

The BDFM has been shown to be promising for a number of applications that require a variable speed drive. The majority of these applications do not need to have servo quality speed or torque control. Many industrial drives in use today use simple open-loop scalar control to vary the shaft speed for a given process. This type of control is much easier and cheaper to implement since it requires no speed feedback to the controller. In the case of induction machine drives, this type of control normally has some speed errors due to slip. This is not a problem, since the feedback to the controller is normally some process variable. In the case of pumps and fans, which are common loads that are now being put on variable speed systems in increasing numbers, the system pressure or flow is the controlled variable in the process; this allows the speed of the machine to be controlled without a costly speed transducer. More costly controllers may include a speed feedback, while still using simple scalar control; these are used in low performance systems, such as in some conveyor belt drives.

The preproduction BDFM drive system discussed here can easily perform the same tasks as the low performance drives listed above. The BDFM lends itself very well

to pump and fan loads because of their limited operating speed range. Pumps and fans both have a cubic power characteristic, so at one half of the rated speed, a maximum of 1/8 of the useful work is being done. The common operation range for these applications is only 2/3 of the rated speed, because non-ideal characteristics and losses all but eliminate the useful work being done at less than 2/3 of the rated speed. The BDFM converter size can be kept small for limited range operation if the machines are optimized for this type of application. The BDFM also has an advantage over low performance drives for conveyor belts in that it operates in a synchronous manner, which eliminates the need for a speed transducer.

It was an easy task to find a number of pumps that have application for a BDFM drive. Cornell Pumps, of Portland, Oregon, manufactures a number of specialized pumps that can be driven at low speed. Most of these pumps are in niche applications that require the movement of solids in a liquid medium. In the 15-20 hp range, models 6NHT and 6NHG are both non clogging pumps designed to run at speeds that would indicate an 8 pole fixed speed machine or some form of reduction gearing with a faster machine[20]. Cornell has some 5 hp pumps designed for use with solids in the pumping medium; these include series 4SCBX (X denoting intake size), which can be used at speeds below 1000 r/min. Models 4SCB4 and 4SCB3 do not suffer large efficiency penalties being run at speeds between 600 and 900 r/min. These two pumps may have uses with a variable speed BDFM drive. Cornell also manufactures a line of pumps designed to move food products such as whole potatoes or small berries in a water medium. These pumps need to run at slow speeds in order not to damage the produce.

Due to the nature of the specialized design, these pumps have very low efficiency. An example pump for this application would be the 6NHP rated at 5 hp at 800 r/min [20].

3.2 Synchronous Operation and Operation Near Loss of Synchronism

In synchronous operation the power winding field is linked to the control winding field via the rotor, allowing for steady power transfer between the stator and shaft. The amount of power and the amount of magnetizing flux provided by each of the stator windings can be controlled by varying the current in the control winding. Depending on the load, at high control current the majority of the magnetizing flux is provided by the control winding. In this condition, the power winding is drawing mostly real power from the utility system. The efficiency of this operating condition is not optimal, since the magnetizing flux for the power winding is supplied by the control winding through the rotor, which adds losses associated with the rotor as well control winding resistance. The efficiency of the machine is much higher when the power and control windings supply their own magnetizing flux. At the high efficiency operating point, the power supplied by the power winding remains approximately constant over the speed range of the machine if the torque is held at a constant level. The control winding power makes up the difference in the power balance by slip power extraction, equivalent to the operation of doubly-fed wound rotor induction machines. At speeds near rated, the control winding current will only be supplying the control magnetizing flux, the resistive loss of the control winding and a portion of the resistive loss in the rotor. At lower

speed, the control winding power will be negative to keep the power balanced, as illustrated in equation (3.1).

$$P_{mech} = speed * torque = P_{power} + P_{control} - P_{losses} \quad (3.1)$$

At low speeds, the control winding power will be the sum of the power needed to balance out the unchanging power winding power and the resistive losses of the control winding. For no load operation, the control power will not go negative over the speed range, since power delivered by the power winding to the rotor is nearly zero; there is some torque component for friction and windage, but these decay as the speed decays. With no power being transferred form the power winding to the rotor, the control winding power will only be making up for the control circuit resistive losses. At higher torque levels, the control winding extracts slip power below the rated speed. The maximum efficiency point will be at control current levels that are near the minimum required to maintain synchronism. With the control winding supplying none of the magnetizing flux for the power circuit, the power winding will draw significant reactive power from the grid. In this condition, the power winding currents will be at their highest synchronous level.

For high torque loads it is desirable to maintain the power winding currents at levels within the rating of the power wiring. To achieve this, the control current can be increased to increase the power factor of the power winding. This condition is not the optimum efficiency point, but it does prevent the power winding from over-heating in machines that have a minimized power winding and extra control winding capacity, such as the lab machine used with the preproduction drive. For operation at rated torque over the entire rated speed range of the lab BDFM, the control winding current magnitude

must be controlled to produce a reasonable balance between the efficiency of the machine and the amount of current flowing in the power winding. At higher loads the control winding current must be at a higher level than the maximum efficiency point to keep the power winding currents at reasonable levels and to ensure that the BDFM maintains synchronism. The magnitude of the control current not only controls the power factor of the power winding, but also affects the stable region of operation.

3.2.1 Waveform characterization of current

As with any machine in steady state, during synchronous operation the power winding current will stay at an approximately constant level if no operating conditions are changed. A sudden increase of the power winding current is a good indication that there is a change in operating condition, such as loss of synchronism. There is some ripple on the power winding current that is associated with the rotor and stator nonlinearities in the preproduction BDFMs. The diecast rotor used employs a caged structure that has been simplified from the ideal BDFM rotor to make it practical for casting [3]. This simplification has removed some connections in the rotor that would provide for more ideal power transfer through the air-gap. Also, the two stator windings share the same back iron and the superposition of control and power winding fluxes will lead to localized saturation effects [4]. Power and control fields travel in opposite directions and the saturation effect appears on the power winding current as low frequency modulation. Figure 3.1 show the steady state power winding current. A sliding window RMS calculated over one period illustrates the fluctuations. Design

changes on the most recent BDFMs have increased the back iron in an attempt to mitigate saturation effects.
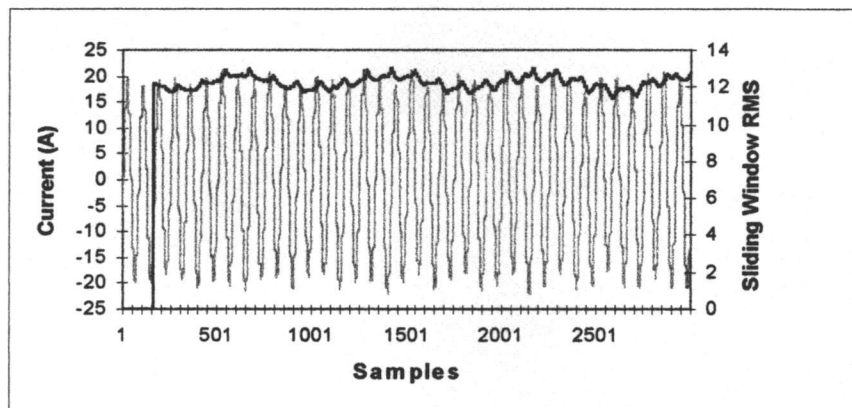
Figure 3. 1 Steady state power winding current in normal operation

Any control strategy that uses the power winding current as an input variable must compensate in some way for the variations of the power current that are inherent in normal operation of a BDFM. The controller developed maintains reasonable power winding currents using a hysteresis band and by sampling over multiple cycles.

It has been shown that the power winding currents maintain approximately stable levels during steady state synchronous operation. Operation when the machine is losing synchronism is notably different. As the machine loses synchronism, the coupling between the control and power windings via the rotor is lost. The BDFM becomes a combination of two independent induction machines sharing the same mechanical rotor and operating at high slip. The currents of the control winding will not show any change during loss of synchronism due to the current forced nature of the inverter. However, power winding current will be affected by loss of synchronism in a predictable manner.

At the onset of loss of synchronism, power winding current will increase significantly, due to higher reactive power requirements in the absence of control winding excitation support and due to the incipient higher slip. Figure 3.2 shows the effect of loss of synchronism on the power winding current. Loss of synchronism occurs at approximately sample number 1750. Again, the RMS of the current is provided for ease of interpretation. The dip in power winding current after loss of synchronism is an effect of the active load that was used to gather this data. Once the machine loses synchronism it will support much less torque and this allows ringing in the torque output of the DC machine that is being used as a load.
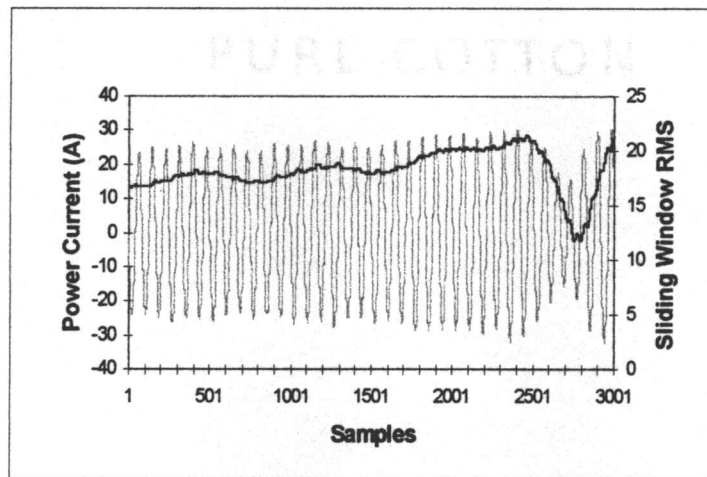
Figure 3. 2 Power winding current during loss of synchronization

3.2.2 Maintaining synchronous operation

The power winding current control of the precommercial drive serves two purposes: it allows the machine to operate at reasonable levels over its entire design

range and it prevents the machine from losing synchronism. To implement this, one

phase of the power winding current is measured using a hall effect current transducer.

The current is sampled 25 times every 60 Hz cycle and all negative readings are inverted.

The signals are then averaged in a sliding window fashion to produce a running average

of power winding current. While this should not be confused with an RMS

measurement, it provides similar information and is extremely simple to implement in a

microprocessor.

$$C_{AVG} = \frac{1}{50} \sum_{X}^{X+50} ABS(C_x) = \frac{2 * C_{peak}}{\pi} \qquad (3.2)$$

This sliding window average current can then by compared to a desired average

current to allow for the control of the system. The desired power winding current is

found during acceptance testing. The maximum power winding current coincides

approximately with the highest efficiency and the lowest permissible value needs to be

higher than the synchronization boundary. The desired band of power currents is set in

the header of the control software and can be changed depending on the load used and

the machine to be controlled. The control current magnitude is changed in accordance

with any deviations in the power winding current. If the power winding current is within

the desired operating band, no change to the control current will be implemented. In the

prototype implementation, power winding currents are regulated in a band between 10

and 12 A rms. This band provides for reasonable efficiency without risking loss of

synchronism. If the power current is above the preprogrammed band, the control current

is increased by a set amount, thus decreasing the power winding current and ensuring

synchronous operation. If the power winding current is below the preset band, the control current will be decreased by a set amount allowing for a more efficient operating point. A ramp controller was implemented for ease of programming and as a simple proof of concept demonstration. Because of the time constants associated with the loads that the pre-production BDFM system encounters, this has proven to be sufficient. If the mechanical load increases in a manner that may cause loss of synchronism, the power winding current will reflect this change and the control winding current will then be varied in a manner that cancels out the increase in power current, thus improving the stability margin of the BDFM. During a speed transition, the BDFM will see an inertial torque which be reflected on the power winding current and cause the control current to be increased to prevent any loss of synchronism. In case these control actions are not sufficient, the controller also monitors for sustained high currents that are seen during loss of synchronism and will shut the system down in a controlled fashion if synchronism is lost.

3.3. Synchronization

The BDFM has a number of features which make it difficult to synchronize. At the locked rotor condition or zero r/min, there is significant transformer coupling through the rotor between the power and control windings. If the control winding is left open circuited and the power winding is exited with 230 V RMS 60 Hz, a voltage of more than 300 V peak is observable on the control winding at start-up and at low rotor speed. The laboratory BDFM also does not function well in low speed operation below 500 r/min.

First, the control winding frequency needs to be more than 26.7 Hz for operation in this speed range. This will significantly limit the control current levels that can be used at low speed since the inverter output becomes voltage limited at frequencies above 26.7 Hz and the limited DC bus voltage. This is a design feature of BDFMs that are optimized for a limited speed range e.g. 600-900r/min in the laboratory drive [4]. Secondly, the laboratory BDFMs that are being used with the controller have diecast rotors, and as was shown in chapter 2, these rotors have a parasitic induction machine characteristic that becomes prevalent at speeds below 600 r/min. It should be noted that this is not a concern under normal operating condition, but hampers low speed operation.

The controller developed for the BDFM allows for acceleration of the machine into its operating range of 600 to 900 r/min with proper synchronization. Synchronous operation at low speeds is not practical and leads to degradation of the machine, so it is not practical to start the machine with 60 Hz on both windings, and accelerate by reducing the control frequency. To accelerate the machine from stand still, the singly fed mode of operation is used. In the case of a caged BDFM rotor, the induction mode torque is significant but with an ideal uncaged BDFM rotor the induction torque is very low as was shown in chapter 2. The cast BDFM rotors have parasitic current leakage paths that were also shown in chapter 2. By using the parasitic induction cage in the BDFM rotors, the machine can be accelerated from stand still in the singly fed induction mode.

The precommercial controller uses the induction mode of the BDFM to accelerate it into the normal operating range and then brings in a control current with a frequency corresponding to the desired synchronization point. This is achieved using contactors on

both the power and control windings and commands to the inverter. A contactor is placed on the control winding to isolate the power electronics in case of failure, and to isolate the inverter from the start-up transients that are seen on the control winding when the BDFM is started in the singly fed induction mode.

For this method of synchronization, the induction mode start up characteristics must be well known for the BDFM and load in question. The characteristics for the laboratory BDFM with an unexcited DC machine as load can be seen in chapter 2. For loads such as pumps and fans, this test must be repeated to determine the startup times necessary for synchronization. For loads with only inertial torque, such as the unexcited DC machine, the minimum control current for synchronization can be very high at low speeds in the operating range. Because of this, the synchronization point for the laboratory BDFM with inertial loads or no load was chosen to be 885 r/min. This allows for minimum synchronization current and allows the timing requirement for synchronization to be more flexible. For load such as pumps or fans which have a square torque speed characteristic ($T \propto \omega^2$), synchronism at lower speeds is practical and desired. The torque characteristics of a pump or fan load make the synchronization of the BDFM with these loads much simpler than no load synchronization.

In this controller the process for synchronization is as follows. With the machine at stand still the power winding contactor is closed. The machine then accelerates in the induction mode. After a predetermined time the inverter is given a frequency command for synchronizing and the control contactor is closed. The control current is then ramped up to near its maximum level to ensure that the machine will synchronize. After a short time period to make sure the machine is fully synchronized, the control current is

then ramped down to normal operating levels and the speed and current controls are enabled [12].

3.4 Speed Control

There are a number of methods for controlling the speed of a BDFM. Open loop constant current control is simple and easy to implement. Since the BDFM is operated in a synchronous manner, no speed feed back is necessary if the machine is always in synchronous operation. It has been show that a large step change in control current frequency will result in oscillations and possible instability in the machine [11]. A closed-loop scalar control was added to improve speed response, and it was shown that the machine speed can be changed at up to 60 r/min per without loss of stability. A slower rate of change was implemented in an open loop fashion for the precommercial drive system. As speed commands are taken from the user interface, the machine control winding frequency is ramped at 2.5 Hz/sec until the desired speed is achieved. This corresponds to 37.5 r/min per sec of speed change.

3.5 Converter-based Power Factor Correction

At the highest efficiency point of operation and low load, the power winding power factor is relatively low, as is the norm with most machines based on induction principles. While power factor of the power winding can be improved by increasing the excitation of the control winding, this is not the only method to improve overall BDFM power factor. It has been shown with high power Flexible AC Transmission Systems

devices that using an active rectifier to inject leading imaginary current into a system can aid in correcting power factor. In the case of a BDFM, the converter needs to have an active front end in order to process the bi-directional power flow from the control winding. For reasons of modularity and manufacturability, the ratings of the inverter and active rectifier are equivalent. When the BDFM operates at maximum efficiency levels, the inverter processes mainly reactive power and the rectifier supplies or extracts minimal power to regulate the DC bus. This leaves a significant amount of reserve capacity in the rectifier that can be used to process leading current and compensate for a power factor problem. During testing of the prototype BDFM, the maximum power processed by the control winding was 700 watts. Since the rating of the rectifier is 3KVA (8 A at 230 V), this allows for a theoretical maximum of 2.9 KVAR of reactive power to be processed by the rectifier at a leading angle of 79° (cos^{-1}(700/3000)). Because of losses in the converter and safety margins this is not realistic. However, angles up to 45° should give more than sufficient margin for proper control of the DC bus voltage. In order to verify the benefits of this form of power factor correction, the controller was implemented to command a 30^0 lead in the rectifier current. This adds a capacitive component to the rectifier current, and compensates a portion of the lagging current in the power winding.

3.6 User Interface

The controller hardware also acts as a host for a user interface. In the current implementation the user interface is an IEE industrial interface panel [21]. Serial

communication is used to pass information to the host controller via a key pad. The terminal also displays any serial communication from the host on a vacuum fluorescent display. The user can press keys to indicate to the host controller to start the machine, stop the machine, increase or decrease speed, and display either the power winding current or the control winding current. The host controller updates the machine speed on the display any time the machine speed is changed. The industrial interface allows the BDFM speed to be controlled from one unit unlike previous BDFM controllers that used a PC as the control interface. The control hardware has provisions that allow for analog speed command signals to be sent to the controller from a remote source such as a PLC; however, this feature is not currently supported in software.

4. Control Implementation

The control implementation for the precommercial BDFM follows the explanation given in chapter 3. The control was implemented using an Intel 80196KC embedded microcontroller, which was adapted from the converter rectifier and inverter controllers with a minimum number of changes. The 80196KC provides an ideal platform for control of this system because of its numerous interface features such as analog to digital converters (ADC), high speed input (HSI), and high speed output (HSO) ports. The software for the controller was developed in a combination of "C" and assembly languages and utilizes a number of software modules that were written for the inverter and rectifier controllers [22]. A users manual is also included in this chapter to be used as reference for set-up and operation. Figure 4.1 show a line diagram of the BDFM control system.

3 Phase
230 V
60Hz

User Interface

8 8 8 8

Contactor

Rectifier

Contactor

Serial HSO

Inverter

Current Measurement

ADC

Contactor

CONTROLLER

BDFM

bi-directional communication

uni-direction communication
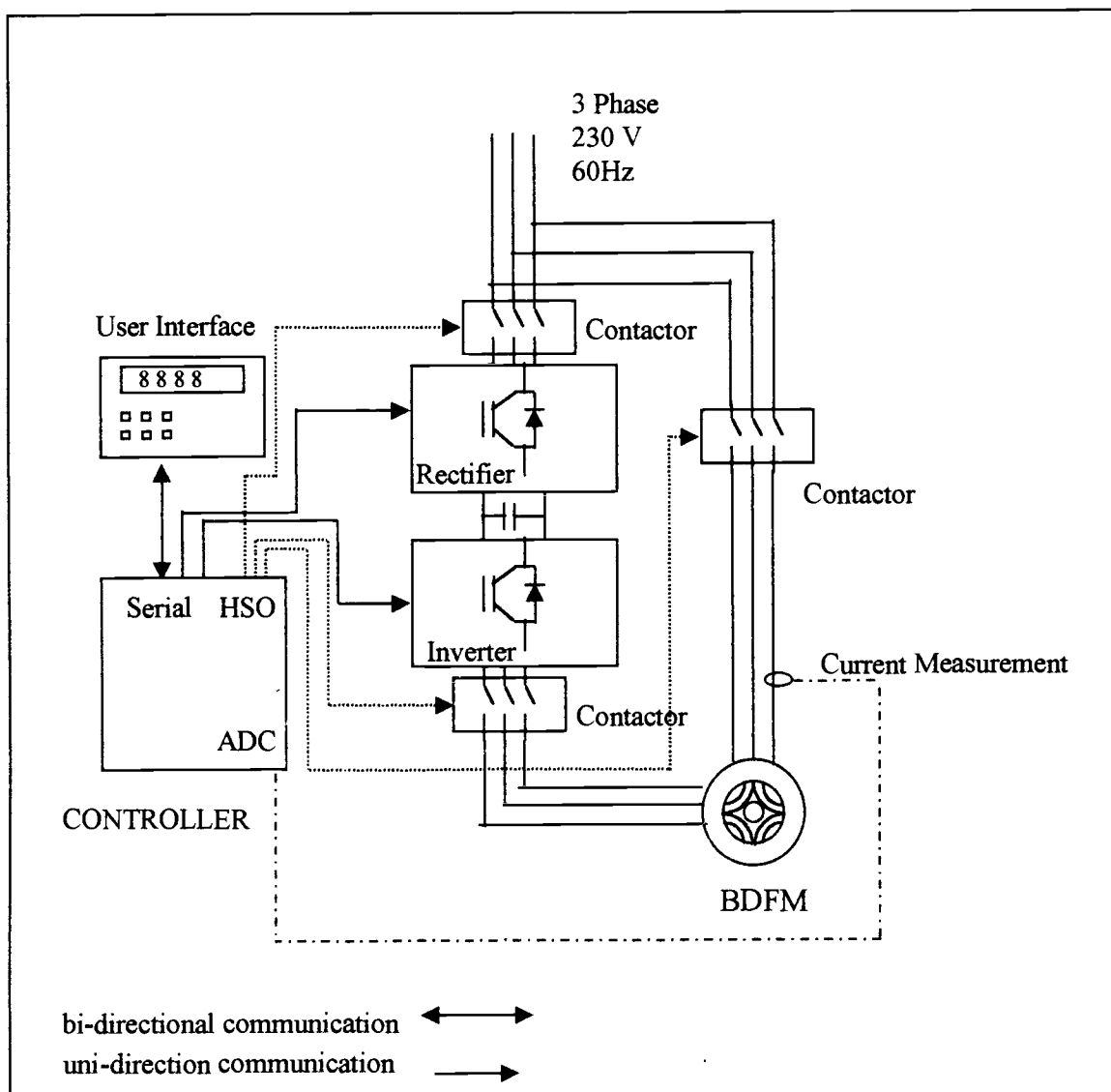
Figure 4. 1 Control system line diagram

4.1 Hardware

The controller uses the same basic hardware as the rectifier and inverter controllers [18]. Some additions were necessary to allow for extra features, e.g. three communication ports. A generalized board was developed by Alex Faveluke to contain

and support the 80196 micro-controller. A detailed description and circuit diagram of this board and its functions is given in [18], and the major characteristics are briefly reviewed here. The microprocessor board is designed with a 16 bit data bus that allows for the fastest mode of information transfer between the EPROM memory and the microprocessor. No exterior RAM is implemented on the board and flash ROM's are used to simplify the transfer of programs to the boards. The boards are clocked at 16MHz and all timing has been developed to operate from this speed. Hardware is included on the board for the use of the eight ADC channels. Each channel is protected by diode clamps and has a small noise rejection filter. Two current transducers are available on the board and may be connected to either an ADC channel or a zero crossing circuit depending on need. If a measurement of a signal zero crossing is needed, a comparator connected to the high speed inputs has been provided. Serial communication to and from the dedicated serial port is passed through a Maxim serial driver chip to allow for communication with standard serial levels. The high speed output module on the 80196 is supplemented by a driver to allow for sinking of higher currents and provides strong pull ups and pull downs.

For the controller implementation described here two changes were made to the control board. One of the current transducers was connected to ADC channel 2 in order to allow for measurement of the power winding current. This current transducer has a rating of 45 A peak. An instantaneous current measurement of 45 A is represented as 9 V by the transducer and a current of -45 A as 3 V. A divider and amplifier scales this output signal into a zero to 5 volt range with zero current being 2.5 volts, for ADC measurement. The ADC has a full range voltage of 0-5 V that corresponds to an output

of 0-1023 or 10 bits. A current of 45 A will cause an output from the ADC of 760. This was the system that was implemented the for use with the converter and should be modified to improve the resolution of the current sensing circuit. Two turns of the power winding feed wire are passed through the transducer window to utilize more of its range, since the maximum normal operating current of the laboratory BDFM is 12 A rms.

Since the controller needs to communicate with three different devices and only one serial port is available on the 80196, high speed output channels 4 and 5 were used for uni-directional serial communication. The HSO port has only a 0-5 V output so a Maxim MAX232 chip was added to the system on an auxiliary board to produce the ±10 volt signal for normal serial communication. The proper configuration for the MAX232 chip can be found in the Maxim products hand book [23]. The HSO "serial ports" are only being used for uni-directional communication so the two receive in pins of the MAX232 should be tied to ground and the two receive out pins should be left floating. These two uni-directional serial channels were used to communicate with the rectifier and inverter controllers, while the dedicated serial port was used to communicate with the host interface. Bi-directional serial communication can be implemented as well if high speed inputs are configured as receivers; this would enable communication of rectifier and inverter status to the user interface. The auxiliary serial port board has .1" center Molex connection to allow for simple connection of the serial lines to the converter control boards [18]. High speed output ports 1, 2, 3 are connected to the contactor controls on the voltage measurement and protection board [18]. HSO channel 1 controls the rectifier contactor, channel 2 controls the power winding contactor and channel 3 controls the inverter contactor.

The user interface for this system consists of an Industrial Electronic Engineers (IEE) integrated entry panel, model number 2 X 20 VIP S03900-A2-A01-07. This panel has to be jumper configured to operate with the control system but no other features other than the labeling of keys need to be programmed or added for it to work with the controller. Power is supplied at a level of 5 volts to the display unit and should be provided in accordance with IEE's recommendations [21]. The interface serial communication is through a standard 25 pin serial connector and the display unit can be set up for a number of different serial modes. The default setup is 9600 baud, odd parity, seven data bits, and one stop bit in a DTE configuration requiring handshaking. The IEE product distribution details the jumpers necessary to change the serial communication to fit a variety of tasks. The controller developed requires 9600 baud, no parity, 8 data bits, and one stop bit with the interface in a DCE configuration.

4.2 Software

The software for this system was developed with both IC96, a processor specific C compiler, and ASM96, the assembler for the 80196. Both compilers were used to create a modular program structure to aid in the development of the system and to allow for the use of existing modules [24]. The complete code listing can be found in Appendix 3. A hierarchy of the program files can be seen in Figure 4.2. The start-up routine was programmed using ASM96 and contains the necessary addressing for the EPROM program to function properly; it also writes the necessary information to a number of special function registers for proper operation of the code on the hardware.

This routine jumps to the main loop of the program which contains the actual control code.
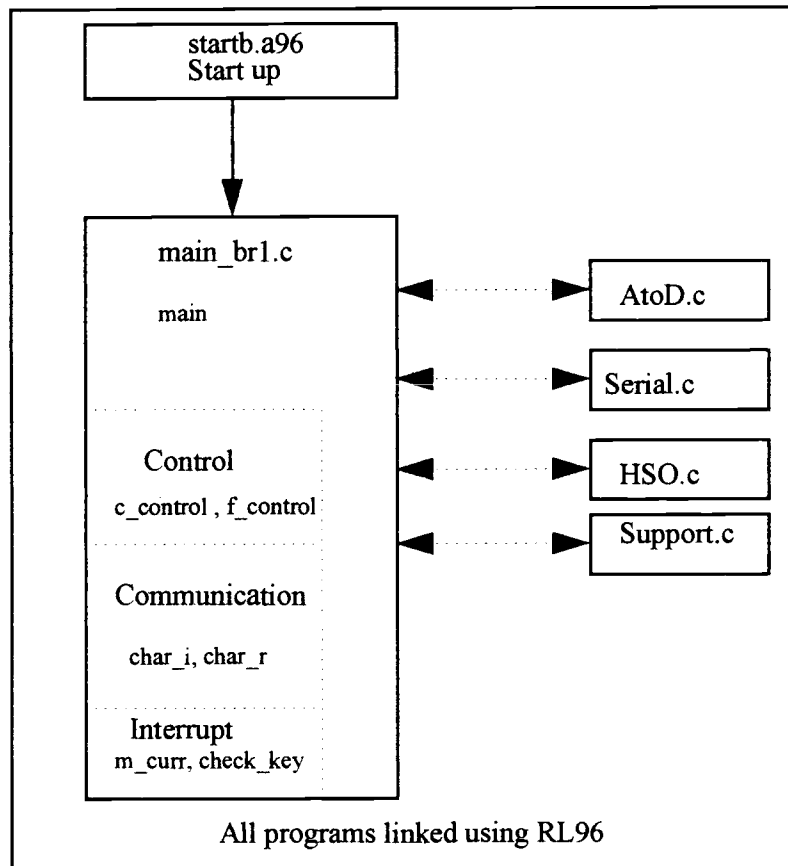
Figure 4. 2 Program hierarchy in the controller

Four preexisting code modules were integrated, including: the HSO module, the ADC module, the serial communication module and the support module. The HSO module has functions pertaining to the high speed output ports. The function *hso_init* initializes the HSO, enables HSO ports 4 and 5 and clears the HSO cam registers, and resets the source timer. The functions *hso_set* and *hso_clear* allow the program to set or

clear any of the 6 HSO ports at approximately the time the function is called. The functions *hso_will_set* and *hso_will_clear* allow the program to set or clear any of the HSO channels at a time after the function is called. The ADC program module contains functions necessary for the operation of the ADC unit in the 80196. This code is contained in the file *atod.c*. The function *atod_int* initializes the ADC to operate in the slow mode of operation and starts timer 2, which is used for other applications [24]. The function *AtoD_Start* starts the analog to digital conversion on the channel that is included in the function call. The function *AtoD_read* waits for a conversion to finish, and passes the results back to the function it was called from. *AtoD_start* should always precede *AtoD_read* or the function will wait indefinitely for a conversion. The file *serial.c* contains three functions that are of interest in this system: *serial_int* which enables the transmit channel and sets the serial communication speed, *putchar* which outputs a passed character on the serial port, and *getchar* which waits for a character to appear on the serial port and returns it. *Support.c* contains other useful functions such a *delayl* which instructs the microprocessor to wait the for the number of milliseconds in the function call. This function was invaluable in programming the synchronization of the BDFM.

The majority of controller code in contained is the file *main_brl.c*. This code contains the *_main* function which calls most other functions and contains the normal operation loop. The header of this file contains the definition statements for the operating parameters of the BDFM, and is where updates to the control system need to be made if the load or machine is changed. This file contains a number of functions used

during the operation of the controller. These are the $c\_control, f\_control, char\_r$,and $char\_i$ functions and the $m\_current$ and $check\_key$ interrupt driven subroutines.

The function $char\_i$ and $char\_r$ both use HSO channels to transmit data serially to the inverter and rectifier controllers, respectively. When called, $char\_i$ takes the character that is stored in the variable ci, and prepares for a serial transmission by clearing HSO pin 5 to indicate a start bit. The function then serializes the character with a bitwise AND to a window variable containing one high bit that corresponds to the serial bit to be sent. The windowing variable begins with the least significant bit set high. If the output of the bitwise AND of the windowing byte and the character variable is zero, the HSO will be commanded to clear after 104 timer ticks (the number of timer ticks for a bit at 9600 baud) after the last HSO operation. Conversely, if the output of the AND is nonzero, the HSO will be set high at the end of the same interval. The windowing bit is then shifted to the right, (multiplied by 2) and the process is repeated for the next bit of the character. This will be repeated for the 8 bits that make up a character. The function ends by commanding the HSO to a high state 104 timer ticks after the last bit was transmitted to produce the stop bit. During these functions the interrupts are disabled to prevent corruption of the transmitted serial string; interrupts are re-enabled on exiting. $Char\_r$ is implemented in an identical manner, except it uses the variable cr.

The $c\_control$ function has the duty of controlling the level of the control winding current during synchronous operation. The $c\_control$ function is called from the $\_main$ function at regular intervals. After a specific number of cycles as set in the header definition, the control begins monitoring the average value of the power winding current. The power winding current control scheme uses one of four possible operations. The

controller will disable the drive if the power winding current is above the fault value set in the header. If the power winding current is above the upper limit of the acceptable band, but below the fault condition, the control current will be increased by an amount set in the file header. If the power winding current is below the acceptable band, the control current will be decreased by the amount set in the header. If the power winding current is acceptable, no change will occur in the control current command. After these checks are completed, any changes to the control winding current command are transmitted to the inverter via the *char_i* function.

The function *f_control* is used to interpret the user commanded speed for the correct control winding frequency. The frequency control function sends an increment or decrement frequency command to the inverter if there is a difference between the previous speed command and the updated speed command. The inverter accepts a 'y' character to increment its frequency reference by .1 Hz, which results in a speed change of +1.5 r/min, and a 'z' character to do the opposite. This function is called every 40 msec, and if continuously changing speed commands are present from the user interface, this will result in speed changes of 37.5 r/min per second. This rate of acceleration is sufficiently slow to allow for the BDFM to stay in synchronous operation during large speed changes.

The *check_char* interrupt driven routine is used to interpret data that is sent to the microcontroller from the user interface. This routine is serviced after any serial input is detected via the receive serial interrupt. The IEE display sends a serial signal whenever the status of a key changes in its switch matrix. An underscore followed by the key number indicates that the referenced key has been pressed. An 'o' character followed by

a key number indicated that the key was released. The key checking routine determines if a valid key command statement is present by first checking for either a valid "key press" or "key release" command, and then setting a status register to indicate to the main program that a key is pressed or no keys are pressed. If the serial buffer does not contain a "key press" or "key release" indicator, the buffer will be placed in a character register for use by the main program loop. The keys 0-4, 6,7 and 8 are supported for specific functions by this control implementation.

The *m_curr* interrupt routine is used to sample the power winding current at fixed intervals and is triggered by an overflow of timer 2. This routine contains the necessary code to create the sliding window average of the power winding current. When this function is called by the interrupt processor, timer 2 is reset so that the function will again be called approximately 1/25 of a 60 Hz current cycle later. The function then increments a pointer variable to the array of previous current measurements or sets this pointer to the first element of the array if the pointer had previously pointed to the last element. The array element that is being pointed to is then subtracted from the sum of 50 current measurements in the array. This produces a sum of the 49 previous measurements by removing the oldest measurement. The ADC module is then commanded to start measuring the output of the current transducer and the system waits for the measurement to complete. If the value of this measurement is below the offset level, corresponding to the zero current level which was measured at startup, the measured value will be subtracted from the offset value, in effect inverting the current measurement and removing the offset. If the current measurement is above the offset value, the offset will be subtracted from the measurement. This produces data that is the

absolute value of the measured currents with no offset component. The processed sample is then added to the sum of previous measurements and divided by the number of samples to produce the average of the power winding current. The measurement is then placed in the array of measured values to be subtracted out after 50 more measurement cycles. Averaging of current is done over two 60 Hz cycles to help reduce noise interference.

The _main function in main_br1.c utilizes all of the previous listed functions to control the BDFM. This function contains the initialization, the synchronization timing, the loop for normal operation, and the shutdown sequence. When this function is called by the startup program after power up, all of the run time variables are initialized and the modular initialization routines are called. After the system is initialized, the processor will wait for the go command from the user interface (key zero). When this key is detected, the processor will start the synchronization process by closing the rectifier contactor. After the DC bus of the converter has fully charged through the diode bridge internal to the switch modules (~1.5 sec), the rectifier is enabled. It takes approximately one second for the DC bus to reach full voltage, after which time the power winding contractor is commanded to close and the machine will accelerate in the induction mode of operation. The processor will then wait for a time period as defined in the header, to enable the inverter at zero current and the preset synchronization frequency. The inverter contactor is then closed and the inverter current is ramped up to the synchronization level. The control current is held at this level for a short period of time to ensure proper synchronization and then ramped down to a normal operating level. The rectifier is then commanded with a leading current angle for power factor correction

and the processor enters the normal operation loop. During this loop, the displayed speed is updated on the user interface if any changes in speed have occurred. The current and frequency control functions are called within this loop. After the control functions are completed, the microprocessor checks the key status registers to determine if any user prompted actions have been commanded. Table 4.1 list the actions that accompany each supported key press.

0Key Press	Commanded Action
key 00 (go)	start the synchronization process
key 01 (stop)	shut the BDFM down
key 02 (^)	increase speed
key 03 (v)	decrease speed
key 06 (Ipav)	display the measured average power current
key 07 (Ic)	display the commanded control current
key 08 (PF)	start power factor correction

Table 4. 1 List of key presses and the associated action

The program will continue in the main loop until a stop command is detected or the current control function detects a fault and commands a stop. After a stop command is detected, the normal operating loop is exited and controller shutdown begins. During shutdown, the power contactor is commanded to open and the inverter is disabled. The machine is then left to spin down with the rectifier still enabled to maintain control of the

DC bus, in case any energy is dumped into the DC bus through the inverter diodes. After one second, all contactors are opened and the program returns to checking for a start command. Figure 4.3 is a flow chart of the main control system.

Control enabled

Start command

Charge DC bus delay

Close 6-pole Contactor

Delay for on the fly synchronization

Command inverter for synchronization
Close inverter contactor

Delay for stable synchronization

Shut down Open contactors
Disable converter

Poll Command register

Speed Control

Delay for machine to stop

Current control
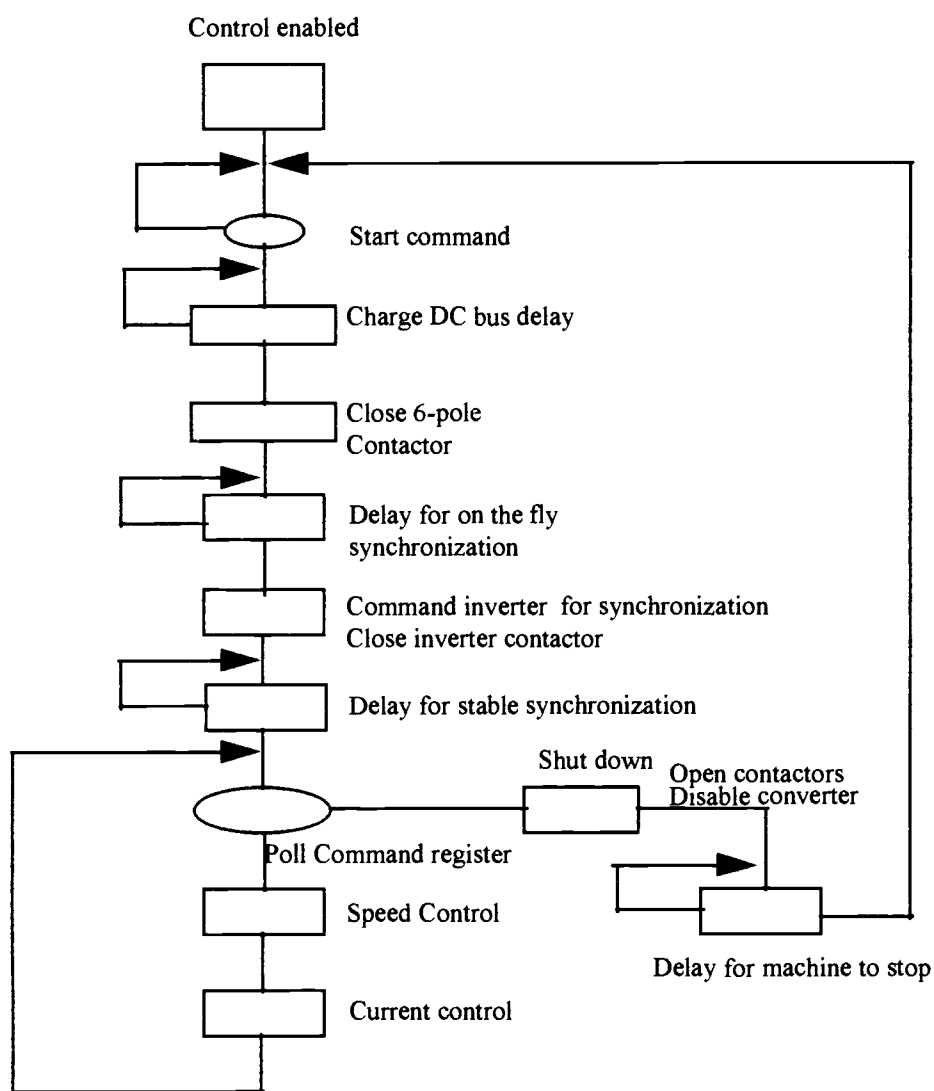
Figure 4. 3 Block diagram of control

4.3 Operation and Set-Up

From an end-user point-of-view, the pre-commercial drive system is very simple to operate, but the set up of a BDFM makes this system more difficult to install. The operating parameters for the BDFM must first be evaluated for a given load and machine, in order for the controller to operate properly. The operating parameters can be estimated by simple field testing and use of machine nameplate data. These parameters must then be added to the control code for programming of a user EPROM, which needs to be inserted into the control board. Following this, the system must be connected to the voltage supply with positive phase sequence which can be determined with a sequence tester for the converter to operate properly.

Once the drive is connected and the proper operating parameters are set, operation is simple. Since the BDFM drive will be delivered as a system that includes the machine, the user setup of the system should be greatly simplified. After applying system power, the black button on the case of the drive must be pressed in order to enable the contactor control hardware. If this button is not pressed before operation is attempted via the controller, the rectifier will see no line voltage or DC bus voltage and go into an error condition that requires power cycling of the converter hardware; moreover, none of the contactors will operate. After the contactor enable button has been pressed, the machine is started by simply pressing the "go" button on the display panel. If all the necessary machine variables were entered correctly, the BDFM will synchronize with no further interactions from the user. Once the BDFM is operating synchronously, speed is displayed on the interface unit and can be varied until a desired

level is reached by pressing and holding either the "⇓" or "⇑" button. If the user wishes to stop the machine, the button labeled "stop" will accomplish this task. Once the converter is disabled by a user input, the user must depress the red mushroom button to discharge the DC bus before the system can be started again [18]. This is to prevent a possible error in the rectifier control, which occurs when the rectifier is enabled with a fully charged DC bus. The contactor supervisory relay has a secondary function of acting as the contactor for the bus bleed resistors. Any time the contactor system is disabled, the bus bleed resistor will be placed across the DC bus to ensure that no charge is left in the bus capacitors. After the DC bus is discharged and the rotor has stopped spinning, the machine can be restarted by following the same procedure outlined above.

For synchronous operation of the BDFM, the power and control winding phase sequences must be opposite. The precommercial converter is equipped with a polarized output plug that contains both the power winding and control winding connections to prevent the two stator windings from being connected with the same phase sequence[18]. The converter is also phase sensitive and will not operate if it is connected with the wrong phase sequence. It should be confirmed that the grid connection of the converter has a positive phase sequence. If it is desirable for the BDFM to rotate in the opposite direction than it was configured for during installation, the phase sequence of both set of windings must be reversed. To accomplish this, two connecting wires on the power windings must be switched as well as swapping to connecting wires on the control windings.

The operating parameters for the laboratory BDFM were found through characterization of the machine in a lab with extensive instrumentation. This procedure

will not work well at field installations because instrumentation is limited, and it is unlikely that a speed transducer will be available to determine the induction mode speed characteristic of a BDFM drive and load. This information is necessary for the synchronization routine to work properly and an alternative method of determining speed utilizes the induction mode and observation of the open control winding voltage. The frequency of the voltage induced on the two pole winding during an induction mode start up can be derived from the steady state synchronous speed equation listed in chapter 1 and repeated here for convenience.

$$f_{mech} = \frac{f_p \pm f_c}{P_c + P_p} \quad \text{or} \quad fc = fp - fmech * (Pc + Pp) \tag{4.1}$$

During an induction mode start, there will be no control winding current but a voltage will be present on the control windings with a frequency that is equal to f_c in Equation 4.1. By using an oscilloscope in the single capture mode it is possible to view the control winding voltage during induction mode run-up. Observation of the varying frequency of this waveform makes it possible to estimate the time it takes for the BDFM to accelerate to a desired speed. This information will allow the user to program the system to synchronize at the proper frequency for a load that cannot be evaluated off-line. To apply this measurement, the control winding feed wires must be disconnected from the machine to separate the converter. Care should be taken in labeling the control wire so that the control winding phase sequence will not be reversed. As a safety precaution, any change in wiring should be done with the converter deenergized. The free end of the wires from the converter should then be insulated to prevent shorting of the inverter outputs during this test. Use of a differential voltage probe is suggested for this test

because the induced control winding voltage can be higher than the rating of most circuit measuring probes. The voltage probe may be connected either line-to-line or line-to-neutral on the control winding; the other terminals need to be isolated with electrical tape during the test. Once the test is prepared as outlined, the normal start-up procedure with the default EPROM settings will energize the power winding and accelerate the rotor close to the 6-pole synchronous speed of 1200r/min. The time it takes for the rotor and load to accelerate to a desired speed can be measured on the time axis of the oscilloscope display by observing the frequency of the control winding voltage. Examples of these run-up curves can be seen in Appendix 1.

The other operating variables for the controller should be provided by machine testing and standard nameplate data. During acceptance testing of a BDFM the points of maximum efficiency for a number of operating conditions should be observed for proper set-up of the current control band. Since the precommerial drive is packaged with a specific machine, the operating parameters should already be programmed into the controller.

Table 4.2 lists the user definable control parameters and the settings for the 5hp prototype. In order to change the operating parameters of the controller for different loads or machines one header in the software must be edited. This header is contained near the top of the file *main_bri.c* , as listed in appendix 2. To update the controller software the file header must first be edited for the new parameters. This file should only be compiled with IC96 because of the hardware specific code included in the file. This code is then linked to the other code modules by RL96, the 80196 specific linker, using directives that are included in the make file listed in appendix 2. The output of the

linking process then needs to be transferred into Intel hex by OH, a hex converter. This hexfile can then be programmed onto EPROM's. The control board is designed to use 28f256 flash ROM's or a compatible programmable ROM. An EPROM program such as EMP20 is necessary to transfer this hex file to the ROM.

Table 4. 2 User definable control parameters

Var. Name	Setting for 5hp Prototype	Explanation
#define F_init	10 (1 Hz)	initial frequency (x10) the converter will produce at synchronization
#define I_init	70 (7 A)	initial control current magnitude (x10) to ensure synchronization
#define F_max	267 (26.7 Hz)	maximum control winding frequency (x10), sets the lower limit of operation
#define F_min	1 (.1 Hz)	minimum control winding frequency (x10), sets the upper limit of operation
#define Syn_D	375 (.375 sec)	run-up time to synchronization in msec minus 200 msec, the current ramp up time (575 -200msec for no load 885 r/min)
#define I_inc	3 (.3 A)	increase in current magnitude if the power winding current is detected above I6_max during current control (x10)
#define I_dec	2 (.2 A)	decrease in current magnitude if the power winding current is detected below I6_mim during current control (x10)
#define I_max	80 (8 A)	maximum control winding current (x10)
#define I_min	20 (2 A)	minimum control winding current (x10)
#define I6_max	92 (Measured average for 12 A rms)	Upper band of the power winding current unscaled from measurement; this is calculated with I6_max=11.4*sqrt(2)*2*Irms/pi (see page 54 for explanation of current measurement)
#define I6_min	83 (Measured average for 10 A rms)	lower band of the power winding current unscaled from measurement this; is calculated with I6_max=11.4*sqrt(2)*2*Irms/pi (see page 54 for explanation of current measurement)
#define I6_fault	120 (16 A rms)	Measured value of the power winding current that will cause the converter to power down under fault conditions

Since the controllers use a 16 bit data bus one EPROM will be programmed with the odd bytes of the code while the other is programmed with the even bytes. Once the EPROM's are programmed they are inserted into the controller board. This is the microprocessor board that is nearest the door opening and has the auxiliary serial board attached to it. The EPROM with the even code bytes is inserted into the memory socket nearest the microprocessor chip. With the new EPROM's in place, the controller is ready to use with the user set operating parameters.

5. Experimental Results

The main goal of this project was to develop a supervisory controller for the BDFM precommerial drive system. This was successfully accomplished, and the outer loop control system performs its designed functions. The controller hardware and software combine to allow a user interface, synchronization of the system, speed control, and power factor correction. This chapter presents some experimental results to illustrate controller performance.

The primary function of the outer loop control system is speed control of the BDFM. As explained earlier, this was implemented using open loop scalar control for a speed response of 37.5 r/min per second. Figure 5.1 shows the response of the BDFM drive system to a change in the speed command, as well as the change in the control winding frequency. As can be seen from the oscilloscope capture, the speed was changed in accordance with the command to decrease speed by 50 r/min in just over 1 second. It may also be noted that no overshoot of the speed is apparent, and the machine stays in synchronous operation throughout the speed change.
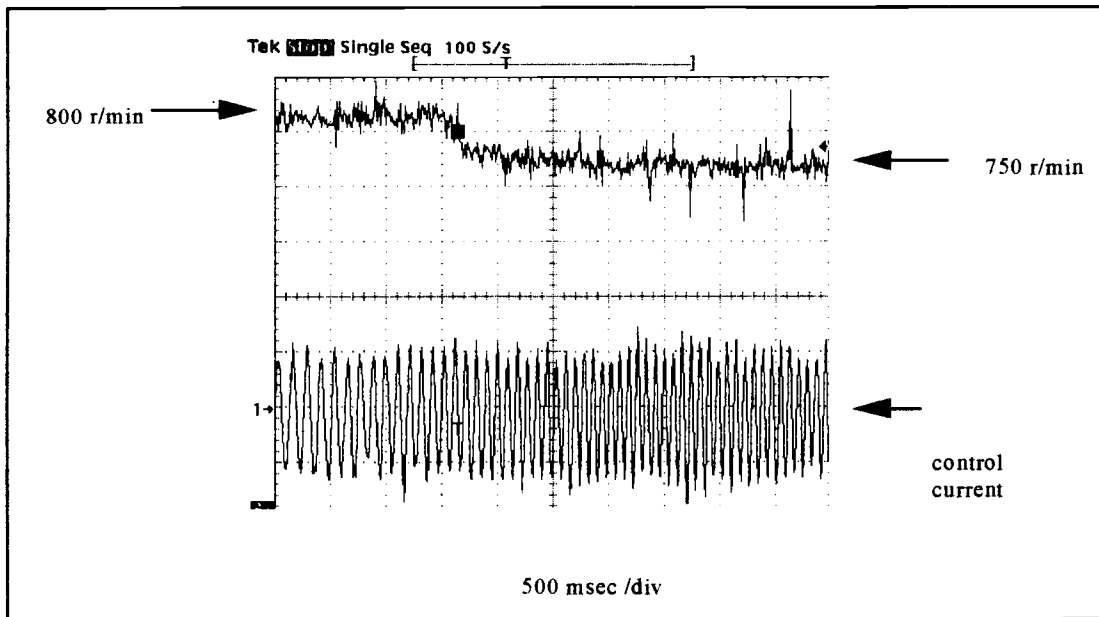
Figure 5. 1 Response to change in speed command

Another primary function of the outer loop controller is synchronization of the BDFM when operation is started. This is accomplished by using the induction mode of operation to accelerate the machine to the desired range of speed, and then commanding a control current that will result in synchronous operation. For an explanation of synchronization timing, refer back to chapters 3 and 4. Figure 5.2 shows a successful synchronization of the machine during no load operation.
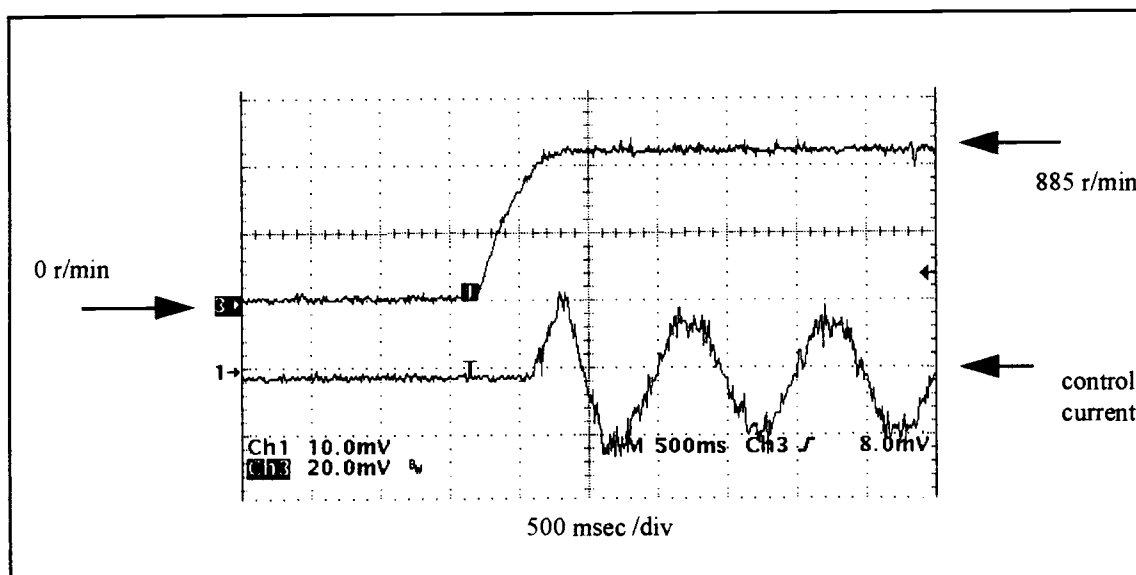
Figure 5. 2 Synchronization of the BDFM (no load operation)

Synchronization at no load is more difficult to achieve than at any other time, because the absence of load torque allows the machine to accelerate very quickly, amplifying any errors in timing. The magnitude of the control winding current must also be greater in order to counteract the parasitic induction effects that are present since there is no load to assist in deceleration. As can be seen from Figure 5.2 the machine accelerates to 885 r/min in ~500 msec. To synchronize the machine at 885 r/min, the control contactor was closed 375 msec after the power winding contactor was closed and the control current was ramped up to a level that allowed for proper synchronization. It may also be observed that there is no overshoot in speed, and that the transition from induction to synchronous operation occurs smoothly.

Active power factor correction was also implemented in a rudimentary form with this controller. During synchronous operation, the rectifier can be commanded to draw

current at a leading angle with respect to the supply voltage. This will allow for some

cancellation of the magnetizing current that is being drawn by the power winding of the

BDFM. Under no load conditions this can be easily observed at speeds near 600 r/min.

Since the control power supplied will be a significant portion of the machine power,

changing the rectifier current angle will have a visible effect on the power winding

current levels. Figure 5.3 shows the input current without power factor correction and

Figure 5.4 displays the results of active power factor correction.
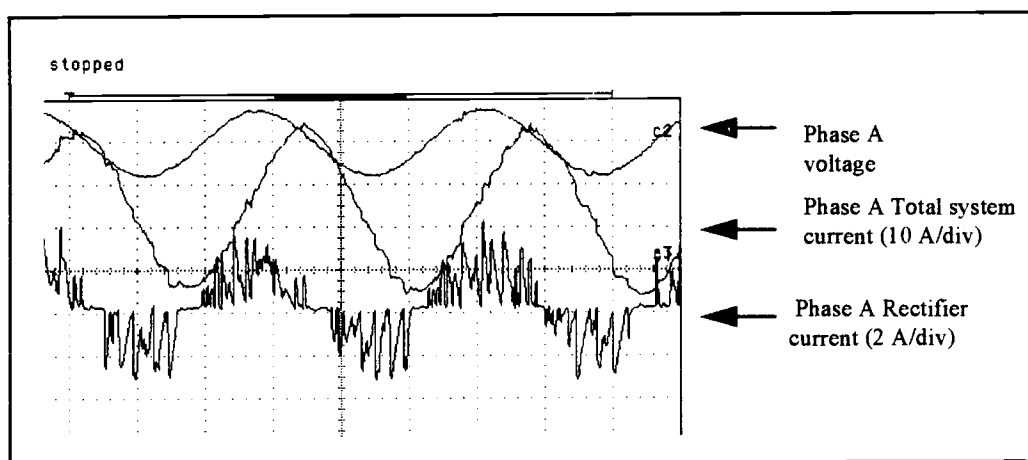
Figure 5. 3   System currents without power factor correction
(600r/min no load 5msec/div time scale)

stopped

Phase A
voltage

Phase A Total system
current (10 A/div)

Phase A Rectifier
current (2 A/div)
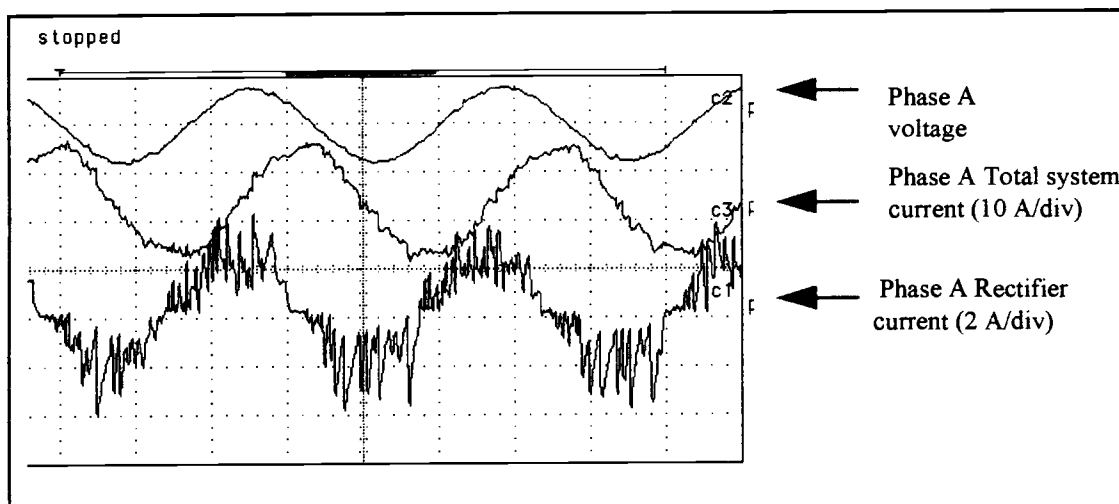
Figure 5. 4 System currents with power factor correction
(600r/min no load 5msec/div time scale)

As can be seen from Figure 5.3, the rectifier current is in phase with the line

voltage and has an approximately sinusoidal shape with a magnitude of less than 2A.

The total system current lags the voltage by a significant margin, and has a magnitude of

near 12A. When the power factor correction is implemented, the rectifier current is

commanded to lead the line voltage by $30°$, which results in a slight increase in the

rectifier current and improvement in the waveform to some extent. The total system

current is reduced, since the leading rectifier current will now be canceling a portion of

the lagging total system current. As was shown in chapter 3, the amount of lead can

theoretically be increased to $78°$ for the prototype system. The power factor correction

at this angle will be more significant and will cancel most of the reactive current that is

being drawn by the system. Because the rectifier is operating significantly below its

rating, there will be significant ripple on the input current [18]. This wave form can be

improved through an increase in the current magnitude by either increasing the phase

lead or increasing the load on the converter[22]. This simple form of power factor correction will actually reduce the power factor during regenerative operation, rather than increase it. For loaded applications within the 600-900 r/min speed range, regenerative operation is common for the converter. During regeneration, the real component of the current will have a phase angle of $180°$. If a lead is commanded to a current with a phase angle of $180°$ it will cause the current to lag. The desire for increased power factor cannot be achieved through the use of the simple power factor correction algorithm during regenerative operation. If bi-directional communication is implemented to the rectifier, a revision to the power factor correction algorithm should be made to correct for the aforementioned shortfall.

During synchronous operation of the system, the control current magnitude is being regulated by the outer loop controller to maintain the power winding current within a pre-set band of operation. For no load operation, outer loop control commanded 2.9 A of control current to achieve a power winding current of 10.5 A at a speed of 885 r/min, while at 600 r/min, 4.9 A of control current were necessary for the power winding current to be maintained at this level. This is because the parasitic induction effect starts to become evident at speeds near 600 r/min and the power winding is supplying power to the parasitic losses, increasing the amount of real power transmitted through the power winding. A control winding current of 4.9 A will improve the power factor of the power winding by supplying a portion of the magnetizing flux, and reducing the power currents to the desired band of operation.

6 Conclusions and Recommendations

For ASD's to become even more prevalent, the cost of these systems must be decreased. The BDFM shows promise as a cost-effective machine for ASD applications. With an integrated control system and diecast rotors this may become a reality. Research on the BDFM has shown that it has merit for this type of application and the prototype developed is suitable for field demonstration and evaluation by drive manufacturers.

A BDFM with a diecast rotor has been shown to work. With some optimization of the casting process, the performance of the diecast rotors will be improved. Simple experimentation with the core insulation of these rotors will improve them enough that they should replace fabricated rotors in future BDFM development. A number of different rotor stack treatments are being investigated to achieve bar-to-stack insulation, which is essential for BDFM operation. Experimental results illustrate the operation of successfully cast BDFM rotors. The results discussed also have application in the manufacturing of induction machines with reduced rotor losses and reduced unbalanced magnetic pull, caused by rotor leakage currents.

The small sample size of this experiment was a major detriment to the castabilty of these BDFM rotors. The density of aluminum in the bars can be increased by experimentation with the gate size and bar shape. More experimentation with the coreplating process may also improve fill and bar-to-stack insulation. With a more in-depth prototype run, the fill of the bars should be able to reach the 91%-95% fill factor typical in the industry. Increasing the fill factor will lower the resistance of the bars, thus

typical in the industry. Increasing the fill factor will lower the resistance of the bars, thus increasing the efficiency of the BDFM. More prototyping should also allow for the investigation of bar shapes which improve the magnetic paths. Current levels in different bars within one nest are unequal, and a grading of bar shape to match the expected current density will improve efficiency. Experimentation on as few as five rotors would pinpoint minimum casting pressure, thereby reducing erosion of the insulation between the rotor bars and stack. After a proper prototype series, an automated casting system should be able to produce BDFM rotors at a rate of one per minute, at approximately the same cost as IM rotors. With these improvements, diecast BDFM rotors should compare as favorably to manufactured rotors, as diecast IM rotors compare to non-diecast IM rotors.

The control system developed fulfills the design requirement to fully integrate a BDFM drive system into one unit. This was accomplished by packaging a bi-directional converter with all of the necessary hardware to operate a BDFM along with an outer loop controller. The controller was shown to operate successfully in this thesis, but a number of features can be updated if development is continued to improve the outer-loop control.

The biggest shortcoming of the control system is the difficulty of changing operating parameters. To make this system more user-friendly, an on-line parameter entering system should be added to the control software that utilizes the remaining keys of the user interface. This will significantly improve the versatility of the system and make it compatible with multiple machines and loads.

The use of standard control theories such as proportional-integral control can also be implemented in the speed and current loops to improve the speed of response of these two control loops.

A feature that would make this system even more universal would be the addition of an analog speed input. This would allow the system to be interfaced with process control systems and increase the applications that this machine can be used on. This can be done by simply adding code to the system to utilize one of the free ADC channels.

The system can be improved further by adding bi-directional communication to the rectifier and inverter to aid in fault checking and allow the outer loop control to do precise control of the active power factor correction that is currently implemented in a simple manner. With the addition of bi-directional communication the controller can then know the direction of power flow and make up for the short comings of the proof of concept power factor correction.

REFERENCES

1. L. J. Hunt, " A New Type of Induction Motor", J. IEE, 1907,V. 39, pp. 648- 667.

2. A. Wallace, R. Spée, H. Lauw, "The Potential of Brushless Doubly- Fed Machines for Adjustable speed Drives", IEEE IAS Pulp and Paper Industry Annual Meeting pp. 45-50, June 1990.

3. P. Rochelle, A. Wallace, R Spée, " Rotor Modeling and Development for the Brushless Doubly- Fed Machine", Conference Record International Conference On Electrical Machines, Aug 1990. .

4. R. Bellagh, " Development of Optimized Brushless Doubly Fed Machines", *Masters Thesis*, Oregon State University, Aug. 1997.

5. B. Koch, R. Spée, B. Clever, " A Comparison Of Stack Preparations Methods For Bar Insulation In Diecast Rotors", Accepted for presentation at the IEEE, IAS Annual Meeting, Oct. 1997.

6. F. Creedy " Some Developments in Multi-Speed Cascade Induction Motors", IEE Proceedings, 1921, V 59, pp. 511-532.

7. A. R. Broadway and L. Burbridge, " Self-Cascaded Machine: A Low Speed Motor or High-Frequency Brushless Alternator", IEE Proceedings. 1970, 117(7), pp. 1277-1290.

8. R. Li, R. Spée, A. K. Wallace and C.G. Alexander, " Synchronous Drive Performance of Bushless Doubly Fed Motors", IEEE, IAS annual Meeting Conference Record, pp. 631-638, 1992.

9. R. Li, R. Spée, and A. K. Wallace, "Determination of Converter Control Algorithms For Stable Brushless Doubly- Fed Drives Using Floquet and Lynaponov Techniques', IEEE PESC Conference Record, pp. 571-577, 1991.

10. B. V. Gorti, G.C Alexander, R. Spée and A.K Wallace, " Characterization of a Brushless Doubly Fed Machine in Current Fed Mode Of Operations" IEEE IA&C, India 1995

11. D. Zhou, "Dynamic Control of Brushless Doubly- Fed Machines", *Doctoral Thesis* Oregon State University, Corvallis OR October 1995.

References continued

12. B. V. Gorti, D. Zhou, R. Spée, G. C. Alexander and A. K. Wallace, " Development of a Brushless Doubly- Fed Machine for a Limited Speed Pump Drive in a Waste Water Treatment Plant", IEEE, IAS Conference Record, 1994.

13. A.K. Wallace , R Spée and G. C Alexander, " The Brushless Doubly- Fed Motor as A Limited Speed Range Pump", IEEE. ISIE, pp. 505-508, Budapest, Hungary 1993.

14. W. Brassfield, R. Spée and T. Habetler, " Direct Torque Control for Brushless Doubly- Fed Machines," IEEE IAS Annual Meeting Conference Record, pp. 615-622, 1992.

15. W. Brassfield, "Direct Torque Control for the Brushless Doubly-Fed machines," *Masters Thesis* Oregon State University, 1993

16. A. Masmoudi, A. Toumi, M.Kamoun and M. Poloujadoff, "Power Flow Analysis and Efficiency Optimization of a Doubly-Fed Synchronous Machine," *Electrical Machine and Power Systems*, Vol. 21, No. 4, 1993, pp. 473-491.

17. Y. Liao, L. Zhen and L. Xu, "Design of a Doubly-Fed Reluctance Motor for Adjustable Speed Drives", IEEE, IAS Conference Record 1994 pp. 305-312.

18. A. Favaluke "Hardware Design and Protections Issues for an AC/AC Converter" *Masters Thesis* Oregon State University, 1997.

19. S. Bhowmik, R. Spée, A.K. Wallace, C. Brune, "Comparison Testing of Equivalent Induction Motor and Brushless Doubly-fed Machine Adjustable Speed Drives." International Conference on Electrical Machines., 1994, pp. 185-190.

20. "Cornell Pump Selection Guide" Cornell Pumps Inc. Portland OR. 1995.

21. "Production Release / E.O. 27955" Industrial Electronic Engineers Inc. Van Nuys California . 1992.

22. S. Bhowmink, "Performance Optimization of Doubly Fed Generation System" *Doctoral Thesis* Oregon State University, Corvallis OR Aug 1997.

23. "Maxim Product Hand Book" Maxim 1995.

24   " 8xC196 KC/ KC User's Manual" Intel 1992.

APPENDICES

Appendix 1   Oscilloscope Captures
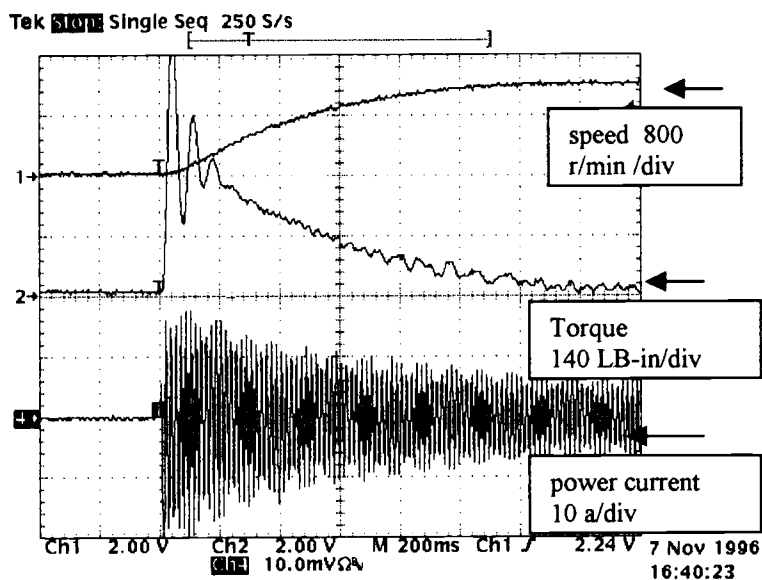
Figure A1.1 open circuit run-up curves (200 msec /div)
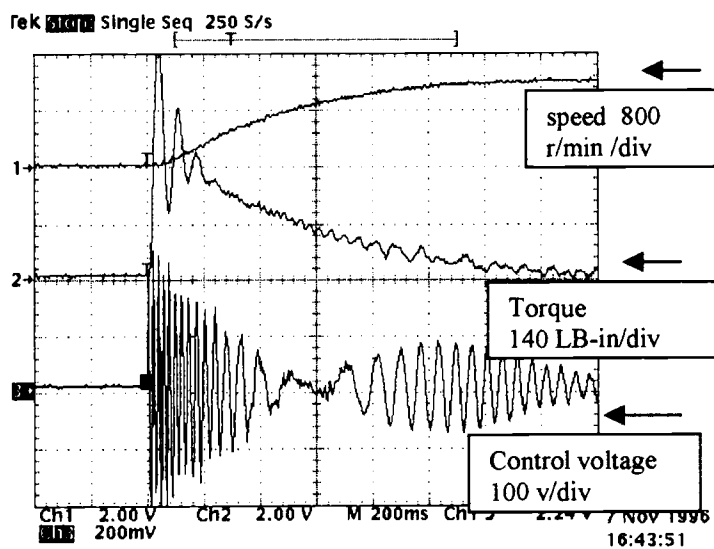
Figure A1.2 open circuit run-up curves (200 msec/div)
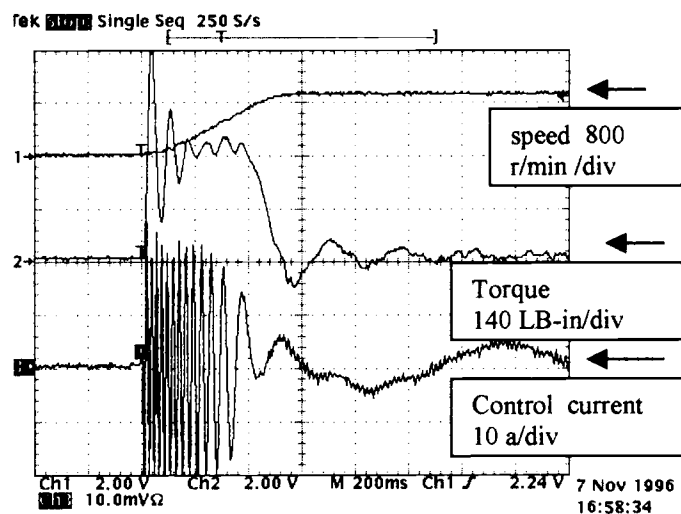
Figure A1.3 closed circuit run-up curves (200 msec/div)
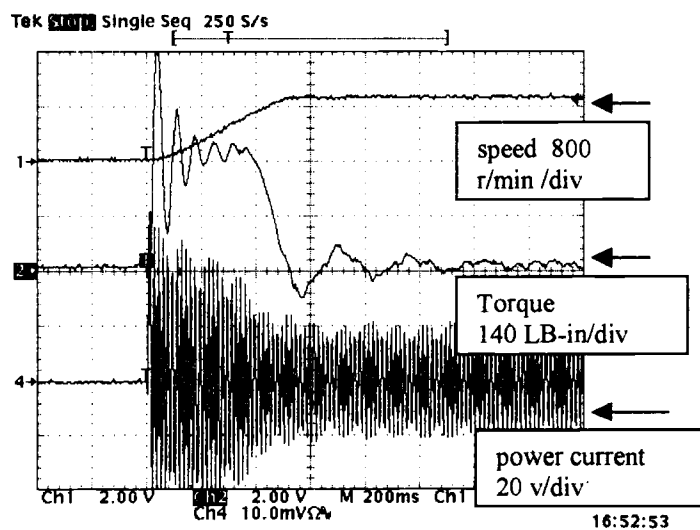
Figure A1.4 closed circuit run-up curves (200 msec/div)
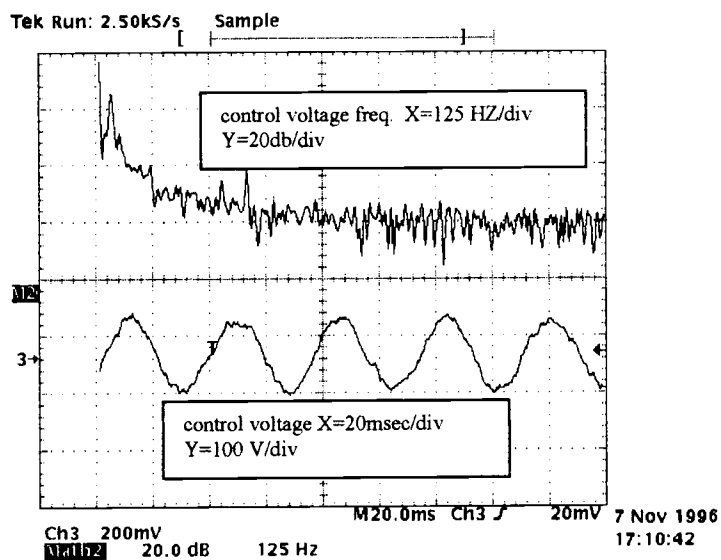
Figure A1.5 open circuit control winding voltage at 500 r/min
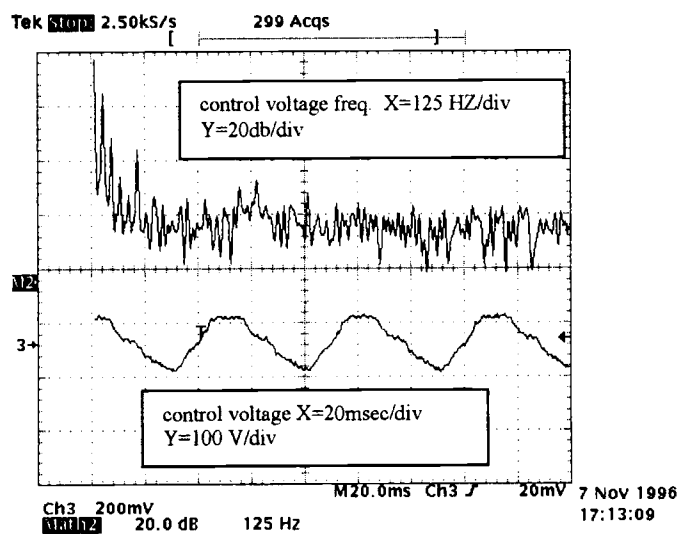
Figure A1.6 open circuit control winding voltage at 600 r/min
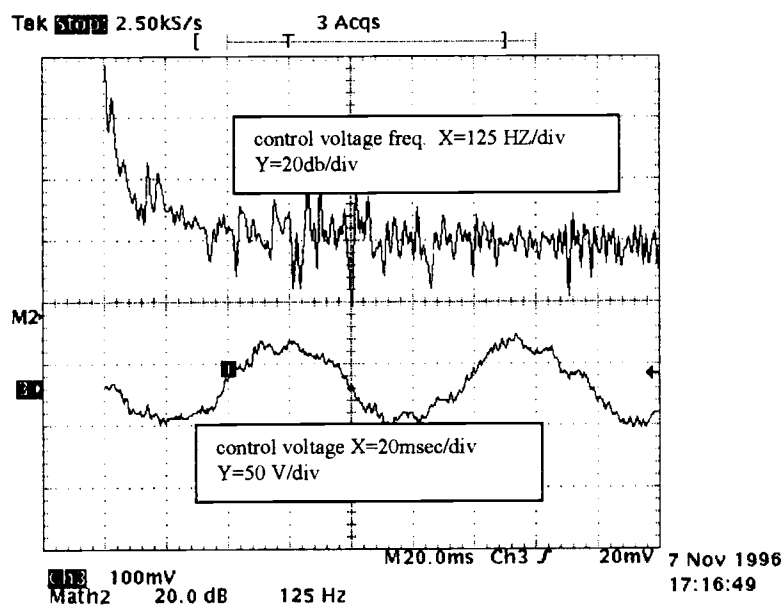
Figure A1.7 open circuit control winding voltage at 700 r/min
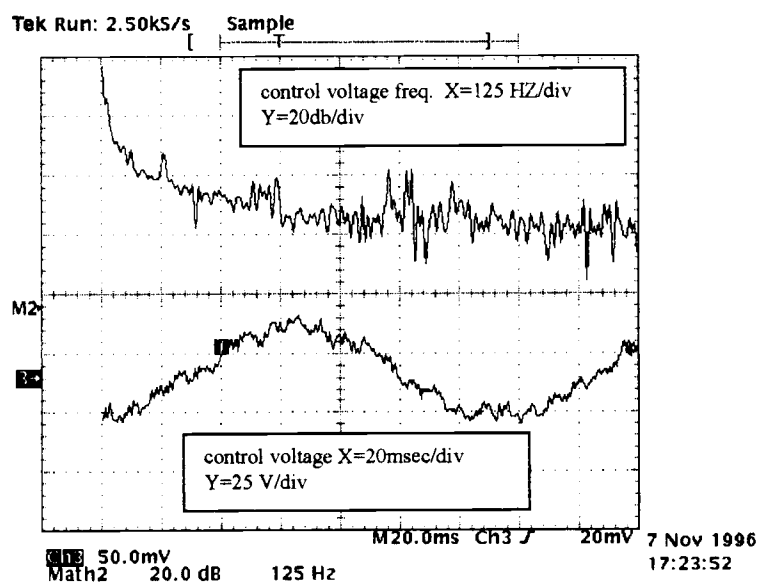
Figure A1.8 open circuit control winding voltage at 800 r/min

Tek Run: 2.50kS/s   Sample

control voltage freq. X=125 HZ/div
Y=20db/div

M2

control voltage X=20msec/div
Y=25 V/div

M20.0ms Ch3 ⌐   20mV   7 Nov 1996
Ch3 50.0mV   17:22:09
Math2   20.0 dB   125 Hz
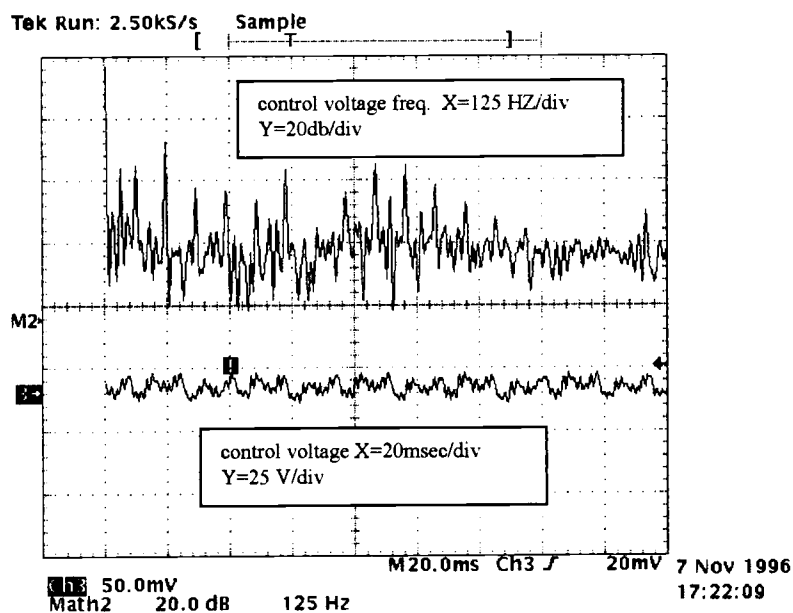
Figure A1.9 open circuit control winding voltage at 900 r/min

Tek Run: 2.50kS/s   Sample

control voltage freq. X=125 HZ/div
Y=20db/div

M2

control voltage X=20msec/div
Y=25 V/div

M20.0ms Ch3 ⌐   20mV   7 Nov 1996
Ch3 50.0mV   17:20:10
Math2   20.0 dB   125 Hz
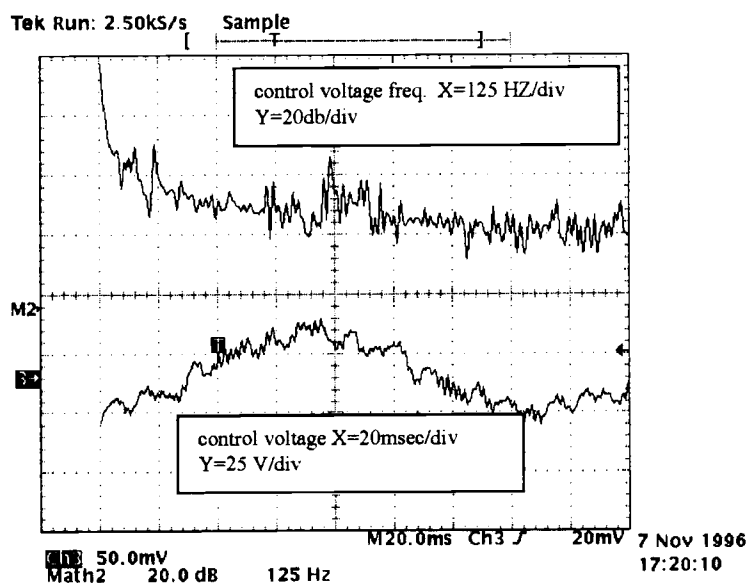
Figure A1.10 open circuit control winding voltage at 1000 r/min

Tek ███ 2.50kS/s ⎯⎯⎯⎯ 103 Acqs ⎯⎯⎯⎯

control voltage freq. X=125 HZ/div
Y=20db/div

M2

control voltage X=20msec/div
Y=25 V/div

M20.0ms   Ch3 ∫   20mV   7 Nov 1996
17:25:04

Ch3 50.0mV
Math2   20.0 dB   125 Hz
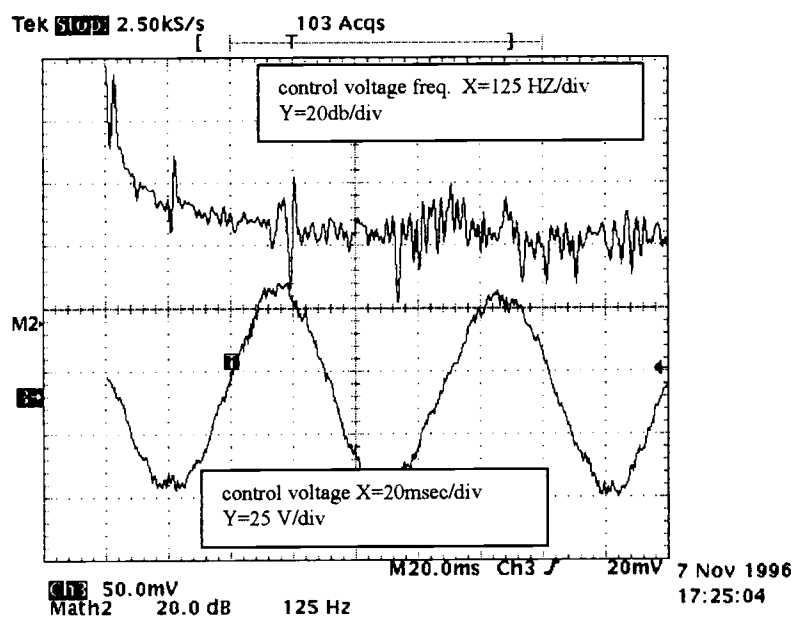
Figure A1.11 open circuit control winding voltage at 1100 r/min

Appendix 2 Program Files

A2.1 Makefile

```
#
☐

☐
startb2.out:    main_br1.obj                \
☐
                startb.obj            \
☐
                hso.obj              \
☐
                atod.obj             \
☐
                support.obj          \
☐
                serial.obj
☐

☐
        rl96  main_br1.obj, hso.obj, support.obj,atod.obj, serial.obj,
startb.obj, c:\ic96\lib\c96.1ib to startb2.out

main_br1.obj:                    ittest.c proto.h 80196.h global.h
        ic96  main_br1.c co li nore sb xr ot(3)

support.obj:                     support.c proto.h 80196.h global.h
        ic96  support.c md(kc) co li nore sb xr ot(3)


startb.obj:                  startb.a96
        asm96   startb.a96


hso.obj:                 hso.c proto.h 80196.h global.h
        ic96  hso.c md(kc) co li nore sb xr ot(3)



atod.obj:                atod.c proto.h 80196.h global.h
        ic96  atod.c md(kc) co li nore sb xr ot(3)



serial.obj:              serial.c proto.h 80196.h global.h
        ic96  serial.c  md(kc) co li nore sb xr ot(3)
```

A 2.2 Main_br1.c

```
/* control program using spot  - Digital Output Commands*/
/* consecpt by Bhanu Gorti */
/* modified by Brian Koch july 97 */
/*last saved 8/15 20:22*/
/*Note: Connect power winding in abc and control winding in acb
directions*/

#include "proto.h"
#include "global.h"
#include "80196.h"
#pragma model(kc)

#define CONT_DELAYI             10/*delay before current control loop*/
#define CONT_DELAYF             100/*delay before frequency control
loop*/

/* digital commands: ixxx /10= current; fxxx /10= frequency*/
/* */
/*SOME OF THE VALUES DEFINED BELOW MAY CHANGE DEPENDING ON OPERATION*/


#define F_init               10 /*1Hz*/
#define I_init                70 /*ramps upto 7A for synchronization*/
#define I_nor                 40 /*4 amps for normal operation*/
#define F_max               267/*26.7Hz; 500 rpm*/
#define F_min               1/*.1Hz; approx. 900 rpm*/
#define Syn_D                 1375/*delay for sychcronization in
                                 msec(true delay -200msec)*/
                            □
#define I_inc                 3/* increase in current magnetude
                                 durring current control*/
                            □
#define I_dec                 2/* decease in current magnetude*/
□
#define I_max               80/*8A;*/
□
#define I_min               20/*2A*/
□
#define I6_max                105      /*11*sqrt(2)*2*i_max/pi)*/
                                 /*non ideal 4.55 instead of 5.55*/
                            □
#define I6_min                90      /*11*sqrt(2)*2*i_min/pi)*/
□
#define I6_fault              130      /**/
□


□
#define S_max               898 /*? plant dependent, speed 898 rpm*/

#define s_min               500 /*? plant dependent, speed 500 rpm*/

/* HSO.3 pin ;  */
#define SHUT_DOWN               0
#define PO_CON                  2
```

```
#define REC_CON              1
#define INV_CON              3
#define DIS                  4
#define REC                  5
#define NO_CHANGE            0

/* defines ADC Module pins */

#define C6                   2
/*#define DON_COM               1
#define UP_COM               2 */
#define VDC                  3


#pragma interrupt(check_key=25)
#pragma interrupt(m_curr=28)
unsigned int iir,winr,bir,timr,cr;
unsigned int iid,wind,bid,timd,ci;
unsigned int i,n,rstat,rstat1; /*counter, status bit*/
unsigned int i2d,f2d,id1,id2; /*variables for control*/
unsigned int I_old,I_new,F_old,F_new,S_old; /*ld control vs*/
unsigned int vstat,vbuss;
unsigned int I_con,S_con,F_con;/*command v*/
unsigned int nn,cn,a1,a2,a3,a4,r1,r2,b1,b2,b3,b4;/*genrel vs*/
/*unsigned int f2temp1,f2temp2,f2temp3; temps*/
unsigned int init1d,init2d,init3d;/*counters*/
unsigned char cr1,cr0,crtemp ;/* comand registers*/
unsigned int curr[50]; /* array of current measurments*/
unsigned int c_avg,ctemp,ctemp1,ato_zero;
unsigned long int c_sum;
/* Must use _main() because main is a reserved word in ASM96 */
void _main() {
        /*initialization of function blocks*/
              AtoD_init();
              PORT_1^=1;
              hso_init();
              PORT_1^=4;
              serial_init();
              PORT_1^=16;
        /*init vaiables*/
              delay1(20);
              PORT_1^=2;
              cn=0;
              TIMER_2=0X7FF0;
slo:          cr1=0xFF;
              cr0=0XFF;
              rstat=0;
              disable();
              INT_MASK_1 |= INT_RI;
/*            INT_MASK_1 |= INT_T2_OVF; */
              enable();
              PORT_1^=1;

              hso_set(REC);
              delay1(1);
              hso_set(DIS);
              delay1(1);
```

```
        putchar('s');
        putchar('t');
        putchar('o');
        putchar('p');      /*not in use state*/
        putchar(13);


        id1=0;
        /* wait until character is received */
        while (!(cr1==0x00))
        {
        PORT_1^=0X02;
        }
        /*while (!(cr1==0x00));*/

        disable();
        INT_MASK_1 |= INT_T2_OVF;
        enable();
        AtoD_start(C6);
        ato_zero=AtoD_read();
        c_sum=0;
        cn=0;
        for( cn=0; cn< 50; cn++)
        {
        curr[cn]=ato_zero;
        c_sum+=ato_zero;
        }
        cn=0;
        rstat=1;
        rstat1=1;
/*close recf contactor and wait 2.5sec*/
        PORT_1^=2;
        hso_set(REC_CON);
        delayl(2500);
/*enable rec*/
         PORT_1^=4;
        cr='E';
        char_r();
        delayl(1);
        cr='N';
        char_r();
        delayl(975);


/*close power contactor wait .25sec*/
        PORT_1^=3;
        hso_set(PO_CON);
        delayl(Syn_D);
/*enable inv*/


            ci='E';
            char_i();delayl(2);
            ci='N';
            char_i();delayl(2);
            ci='i';
            char_i();delayl(2);
```

```
                          ci='0';
                          char_i();delay1(2);
                          ci='0';
                          char_i();delay1(2);
                          ci='0';
                          char_i();delay1(2);
                          ci='f';
                          char_i();delay1(2);
                          ci='0';
                          char_i();delay1(2);
                          ci='1';
                          char_i();delay1(2);
                          ci='0';
                          char_i();delay1(2);

                 I_old=40;
                 F_old=10;
                 S_con=999;
                 F_con=10;
                 S_old=000;
/* set the inverter contactor*/
                 hso_set(INV_CON);
                 for(nn=0;nn<70;nn++)
                  {
                   ci='w';
                   char_i();
                   delay1(1);
                  }
                 ci='i';
                 char_i();
                 delay1(2);
                 ci='0';
                 char_i();
                 delay1(2);
                 ci='7';
                 char_i();
                 ci='0';
                 char_i();
                 delay1(25);


                 for(nn=0;nn<30;nn++)
                  {
                   ci='x';
                   char_i();
                   delay1(3);
                  }
                 ci='i';
                 char_i();
                 delay1(2);
                 ci='0';
                 char_i();
                 delay1(2);
                 ci='4';
                 char_i();
                 ci='0';
                 char_i();
```

```
            delayl(2);


/*runs while run statis is 1*/

        while ((rstat&&rstat1)!=0){
            iccontrol();
            fccontrol();
            PORT_1^=0X0A0;
            S_con=(600-F_con)*15/10;
            if(S_con != S_old)
            {
                    a1=S_con/1000+48;
                    r1=S_con%1000;
                    a2=r1/100;
                    r2=r1%100;
                    a3=r2/10;
                    a4=r2%10;


                    putchar(a1);delayl(5);
                    putchar(a2+'0');delayl(5);
                    putchar(a3+'0');delayl(5);
                    putchar(a4+'0');delayl(5);
                    putchar(13);
             }
            delayl(30);



        S_old=S_con;      /*save old speed*/
      /* check serial port*/
      /*            while( !(SP_STAT & SP_RI) );
            cr0=SBUF;
            while( !(SP_STAT & SP_RI) );
            cr1=SBUF;                     */


            if  ((cr1==0x02)&&(cr0==1))
            {
                    PORT_1^=0X40;
                    F_con--;
                    rstat=1;
                    if(F_con<=F_min)
                    {
                    F_con=F_min;
                    }
            }
            else if ((cr1==0x03)&&(cr0==1))
            {
                    PORT_1^=0X20;
                    F_con++;
                    rstat=1;
                    if (F_con>=F_max)
                    {
                    F_con=F_max;
                    }
```

```
        }
        else if ((cr1==0x04)&&(cr0==1))    /* DC Bus Check*/
        {
            cr0=0;
            PORT_1^=7;
            AtoD_start(VDC);
            vstat=AtoD_read();
            vbuss=vstat/2;

            a1=vbuss/1000+48;
            r1=vbuss%1000;
            a2=r1/100;
            r2=r1%100;
            a3=r2/10;
            a4=r2%10;
            putchar(0x1b);
            putchar(0x06);
            putchar('V');delayl(5);
            putchar(a1);delayl(5);
            putchar(a2+'0');delayl(5);
            putchar(a3+'0');delayl(5);
            putchar(a4+'0');delayl(5);
            putchar(13);
            rstat=1;

        }
        else if   ((cr1==0x06)&&(cr0==1))/*((cr1==0x06)&(cr0==1))*/
/* curr check*/
        {
            cr0=0;
            PORT_1^=0X080;

            a1=c_avg/1000+48;
            r1=c_avg%1000;
            a2=r1/100;
            r2=r1%100;
            a3=r2/10;
            a4=r2%10;
            putchar(0x1b);
            putchar(0x06);
            putchar('c');delayl(5);
            putchar(a1);delayl(5);
            putchar(a2+'0');delayl(5);
            putchar(a3+'0');delayl(5);
            putchar(a4+'0');delayl(5);
            putchar(13);
            rstat=1;
        }
        else if   ((cr1==0x08)&&(cr0==1))    /* set power facture
correnction*/
        {
            cr0=0;
            cr='L';
            char_r();delayl(2);
            cr='3';
            char_r();delayl(2);
            cr='2';
```

```
                    char_r();delay1(2);
                    cr='5';
                    char_r();delay1(2);
                    putchar('&');



            }
            else if  ((cr1==0x07)&&(cr0==1))/*((cr1==0x06)&(cr0==1))*/
/* curr check*/
            {
                    cr0=0;

                    a1=I_new/100+48;
                    r1=I_new%100;
                    a2=r1/10;
                    a3=r1%10;

                    putchar(0x1b);
                    putchar(0x06);
                    putchar('I');delay1(5);
                    putchar(a1);delay1(5);
                    putchar(a2+'0');delay1(5);
                    putchar(a3+'0');delay1(5);
                    putchar(13);
                    rstat=1;
             }

            else if (cr1==0X01)
            {
                    rstat=0;
            }
            else
            {
                    rstat=1;
            }
}                                  /*end main while lo*/

/*start of shut down*/

 /*          disable inverter */
             PORT_1=0;
            hso_clear(PO_CON);
            ci='d';
            char_i();

             delay1(1000);
            cr='d';
            char_r();
             delay1(1000);
            hso_clear(INV_CON);
            hso_clear(REC_CON);
            goto slo;


}
iccontrol()  {
```

```
        if(id1 < CONT_DELAYI)
        {
                id1+=1;
                I_new = 40;
        }
        else
        {
                if (c_avg > I6_fault)
                {
                rstat1=0;
                }
                if (c_avg< I6_min)
                {
                I_new=I_old-I_dec;
                }
                else if (c_avg > I6_max)
                {
                I_new= I_old+I_inc;
                }
                if (I_new>I_max)
                {
                I_new=I_max;
                }
                if (I_new<I_min)
                {
                I_new=I_min;
                }
        }
/* current command process*/
        if (!(I_new == I_old))
        {

                b1=I_new/100+'0';
                b2=I_new%100;
                b3=b2/10;
                b4=b2%10;

                ci='I';
                char_i();delay1(1);
                ci=b1;
                char_i();delay1(1);
                ci=b3+'0';
                char_i();delay1(1);
                ci=b4+'0';
                char_i();delay1(1);
        }
        I_old=I_new;
    }


fccontrol()  {
        /*frequency unchanged during synchronization*/
        if (n < CONT_DELAYF)
        {
        n+=1;
        F_old=F_init; /*synch at 899 rpm*/
        }
        else
```

```
                {

/* check F_con and F-old*/
                if (F_con < F_old)
                {
                    F_old-=1;
                    ci='z';
                    char_i();
                }
                else if (F_con > F_old)
                {
                    F_old+=1;
                    ci='y';
                    char_i();
                }
                else
                {
                    F_old=F_con;

                }
                /*putchar(10);
                putchar(32);*/

}
}
char_i()
{
        disable();
        iid=0;
        timd=TIMER_1+104;
        hso_will_clear(DIS,timd);
        wind=1;
        for(iid=0;iid<8;iid++)
        {
                timd=timd+104;
                bid=ci&wind;
                if (bid!=0)
                    {
                    hso_will_set(4,timd);
                    }
                else
                    {
                    hso_will_clear(4,timd);
                    }
                wind=wind*2;
        }
        timd=timd+104;

        hso_will_set(4,timd);
        init2d=2000;
        do
        {
        init2d--;
        }
        while(init2d>1);
        enable();
}
```

```
char_r()
{
        disable();
        iir=0;
        timr=TIMER_1+104;
        hso_will_clear(REC,timr);
        winr=1;
        for(iir=0;iir<8;iir++)
        {
                timr=timr+104;
                bir=cr&winr;
                if (bir!=0)
                    {
                     hso_will_set(REC,timr);
                     }
                else
                    {
                     hso_will_clear(REC,timr);
                     }
                winr=winr*2;
        }
        timr=timr+104;

        hso_will_set(REC,timr);
        init3d=2000;
        do
        {
        init3d--;
        }
        while(init3d>1);
        enable();
}
void check_key()
{
        disable();
        crtemp=SBUF;
    /*  putchar(crtemp);*/
        if   (crtemp==0x5F)
        {
                cr0=1;
                /*  cr1=getchar();*/
        }
        else if (crtemp==0x6F)
        {
                cr0=0;
                /*   cr1=getchar(); */
        }
        else
        {
        cr1=crtemp;
        }
        enable();

    }

  void m_curr(){
```

```
disable();
cn++;
if (cn>49)
{
        cn=0;
        PORT_1^=2;
}

c_sum-=curr[cn];
AtoD_start(C6);
ctemp=AtoD_read();
if (ctemp<=ato_zero)
{
        ctemp1=ato_zero-ctemp;
        curr[cn]=ctemp1;
        PORT_1^=8;
}
else
{
        ctemp1=ctemp-ato_zero;
        curr[cn]=ctemp1;
        PORT_1^=4;
}
c_sum+=curr[cn];
c_avg=c_sum/50;
PORT_1^=16;
TIMER_2=0X7DB0;
enable;
/* reset a timer*/
  }
```

A 2.3 Atod.c

```c
#include "proto.h"

#include "80196.h"

#include "global.h"


void AtoD_init()
{
        char ioc;

/*      read options
*/
        WSR = 15;
        ioc = IOC2;
        WSR = 0;

/* Enable A/D Clock prescaler */
        ioc &= ~AD_NOT_PRESCALE;
        ioc |= T2ALT_INT;
        ioc &= ~T2UD_ENA;
        ioc &= ~FAST_T2_ENA;
        IOC2 = ioc;
/* added by brian koch 7.19.97 for an internal source for timer 2*/
        WSR = 15;
        ioc= IOC0;
        ioc &=~T2RST_ENA;
        WSR =0;
        IOC0= ioc;
        WSR = 1;
        ioc=IOC3;
        ioc |= T2_ENA;
        ioc &= ~CLKOUT_DIS;
        ioc &= ~RESV_IOC3;
        IOC3= ioc;
        WSR =0;
}


/* A to D start
        initiate conversion
*/
void AtoD_start(channel)
int channel;
{
        AD_COMMAND = channel | AD_GO;
}

/* A to D read
        Wait for conversion to finish before reading.
*/
unsigned int AtoD_read()
{
        unsigned int result;
```

```
        while( AD_LOW & AD_BUSY )
                ;

        result = AD_LOW;
        result += AD_HIGH*256;
        result >>= 6;

        return( result );
}
```

A 2.4 Hso.c

```c
#include "proto.h"

#include "80196.h"


void hso_init()

{

      char ioc;

      int i;


/* enable all high speed outputs

*/

      WSR = 15;

      ioc = IOC1;
      WSR = 0;
      ioc |= ( HSO_4_ENABLE | HSO_5_ENABLE );
      IOC1 = ioc;

/* disable cam locks and clear
*/
      WSR = 15;
      ioc = IOC2;
      WSR = 0;
      ioc |= HSO_CAM_CLEAR;
      ioc &= ~HSO_LOCK_ENABLE;
      IOC2 = ioc;

/* reset timer 1 which will be used as source
*/
      WSR = 15;
      TIMER_1 = 0;
      WSR = 0;

}


/* hso set
      Turn on.
*/
void hso_set( channel )
int channel;
{
      while( IOS0 & HSO_HOLDING_FULL )
            ;
```

```
        HSO_COMMAND = channel | HSO_SET;
        HSO_TIME = TIMER_1 + 2;
}


/* hso clear
        Turn off.
*/
void hso_clear( channel )
int channel;
{
        while( IOS0 & HSO_HOLDING_FULL )
                ;
        HSO_COMMAND = channel;
        HSO_TIME = TIMER_1 + 2;
}


/* hso will set
        Schedule turn on.
*/
void hso_will_set( channel, t )
int channel;
unsigned int t;
{
        while (IOS0&HSO_HOLDING_FULL)
                ;
        HSO_COMMAND = channel | HSO_SET;
        HSO_TIME = t;
}


/* hso will clear
        Turn off.
*/
void hso_will_clear( channel, t )
int channel;
unsigned int t;
{
        while (IOS0&HSO_HOLDING_FULL)
                ;
        HSO_COMMAND = channel;
        HSO_TIME = t;
}


void hso_wait(pin)
int pin;
{
        unsigned int bit;

        bit = 1 << pin;

        while ( !(IOS0 & bit) )
                ;

}


void hso_will_reset(t)
unsigned int t;
{
```

```
        HSO_COMMAND = HSO_TIMER_RESET | HSO_TIMER;
        HSO_TIME = t;
}
```

A 2.5 Serial.c

```c
#include "proto.h"
#include "80196.h"
#include "global.h"

/* serial initialization */

serial_init()

{

char iocl;

/* baud rate = (crystal frequency/(64*(B+1))
   load rate sequentially, low byte first
   most significant bit determines source */

/*BAUD_RATE=BAUD_LOW;
BAUD_RATE=BAUD_HIGH | BAUD_XTAL1;*/

BAUD_RATE=0x67;
BAUD_RATE=0x80;
/* clear 9th data bit
   enable the receiver
   disable parity
   set mode 1 (standard asynchronous) */
WSR = 0 ;
/*SP_CON=SP_REN + SP_PEN + SP_MODE_1;*/
SP_CON=SP_REN + SP_MODE_1;
/*SP_CON=SP_MODE_1;*/

/* enable TXD pin */

WSR=15;
iocl=IOC1;
WSR=0;
IOC1=iocl | TXD_ENABLE;
}

/* spchk
   check serial port for received character */

int spchk()
{
return(SP_STAT & SP_RI);
}

/* getchar
   get character from the serial port
   uses polled operation */

int getchar()
{
/* wait until character is received */
```

```c
while( !(SP_STAT & SP_RI) )
     ;
return(SBUF);
}

/* get word
    get a word from serial port */
unsigned int getw()
{
unsigned int w;
w=getchar();
w+=getchar()*256;
return(w);
}

/* putchar
    put a character into the serial port */
int putchar(c)
unsigned char c;
{
int x;
/* wait until buffer empty */
while(!(SP_STAT & SP_TXE))
     ;
WSR = 0 ;
SBUF=c;

for ( x=0 ; x<100 ; ++x)
    ;
return(c);
}

/* puts
    put a string to the serial port
int puts(s)
char *s;
{
int c;
while (*s){
c=*s;
if (putchar(c)!=c)
    return(0);
++s;
}
return(1);
}

putw
    put a word to the serial port
unsigned int putw(c)
unsigned int c;
{
putchar(c%256);
putchar(c/256);
return(c);
}
                                    */
```

A 2.6 Support.c

```c
#include "proto.h"

#include "80196.h"

/* delays
      delay by number of timer 1 clocks (us)
*/
void delays( n )
unsigned int n;
{
      unsigned int now;
      unsigned int end;

      now = TIMER_1;
      end = now+n;

      if (end<now) {
            /* wait for rollover first */
            while(TIMER_1 > end)
                  ;
      }
      while(TIMER_1 < end)
            ;
}

/* delayl
      delay by number of 1000 * timer1 clocks (ms)
*/
void delayl( n )
unsigned int n;
{
      while (n--) {
            delays(1000);
      }
}
```